Dissection of the Eyelid and Orbit with Modernised Anatomical Findings

Hirohiko Kakizaki[*,1], Seah Lay-Leng[2], Ken Asamoto[3], Takashi Nakano[3], Dinesh Selva[4] and Igal Leibovitch[5]

[1]*Department of Ophthalmology, Aichi Medical University, Nagakute, Aichi 480-1195, Japan*

[2]*Singapore National Eye Centre, 11 Third Hospital Avenue, 168751, Singapore*

[3]*Department of Anatomy, Aichi Medical University, Nagakute, Aichi 480-1195, Japan*

[4]*South Australian Institute of Ophthalmology and Discipline of Ophthalmology & Visual Sciences, University of Adelaide, South Australia, Australia*

[5]*Division of Oculoplastic and Orbital Surgery, Department of Ophthalmology, Tel-Aviv Medical Center, Tel-Aviv University, Tel-Aviv, Israel*

Abstract: Sufficient knowledge of eyelid and orbit anatomy is essential for achieving optimal functional and cosmetic results in ophthalmic plastic and reconstructive surgery. Utilizing the surgical techniques used *in vivo* can result in difficulties in correct exposure and identification of structures in cadavers. Therefore, special techniques are required to perform appropriate post-mortem anatomical dissections of the eyelid and orbit. In addition, as the number of cadavers for teaching and dissections is very limited, systematic anatomical dissections will maximize their efficient utilization. Here, we present detailed techniques of eyelid and orbital dissections with modernized anatomical findings for anatomists as well as ophthalmologists, focusing on preparation for dissection, dissection of the upper and lower eyelids, handling of the conjunctival fornix, the medial and lateral canthi, and identification of extraocular muscle insertions.

INTRODUCTION

Sufficient knowledge of eyelid and orbit anatomy is essential for achieving optimal functional and cosmetic results in ophthalmic plastic and reconstructive surgery. Utilizing the same surgical techniques used *in vivo* can result in difficulties in correct exposure and identification of structures in cadavers. Therefore, special techniques are required to perform appropriate post-mortem anatomical dissections of the eyelid and orbit.

In this manuscript we use a Japanese male cadaver aged 83 years old at death and fixed in 10% buffered formalin. We present a detailed description of the dissection techniques of the eyelid and orbit with modernised anatomical findings. Most of the vascular and nerve dissections were omitted as they usually need a different specimen for dissection.

The cadaver was registered with Aichi Medical University, and proper consent and approval were obtained prior to use. Methods for securing human tissues were humane, and complied with the tenets of the Declaration of Helsinki.

1. Preparation for Dissection and Exposure of the Orbicularis Oculi Muscle

A. The dissection area is first marked with a fine tip marker (Fig. **1-1**).

The dissection area borders are marked in 4 points; upper: supra-brow, medial: 2mm lateral to the mid-facial line, inferior: same height as the ala nasi, lateral: 15 mm lateral to the lateral border of the lateral orbital wall. The medial border of the dissected area extends the lower and upper orbital rims, but does not reach the ala nasi. Next, a horizontal line is drawn from the medial point to the lateral point. This line splits into two lines passing about 2 mm from the upper and lower eyelid margins. A vertical line is drawn from the upper and lower points to the centre of the horizontal eyelid lines.

Fig. (1-1). The dissection area is first marked with a fine tip marker.

*Address correspondence to this author at the Department of Ophthalmology, Aichi Medical University, Nagakute, Aichi 480-1195, Japan, Tel: +81-561-62-3311, Ext. 2181; Fax: +81-561-63-7255;
E-mail: cosme@d1.dion.ne.jp

1877-6094/10

B. Superficial skin incisions are made along the marked lines (Fig. **1-2**)

The skin is meticulously detached from the underlying orbicularis oculi muscle (OOM) starting from the eyelid margin and using Westcott scissors (Fig. **1-3**).

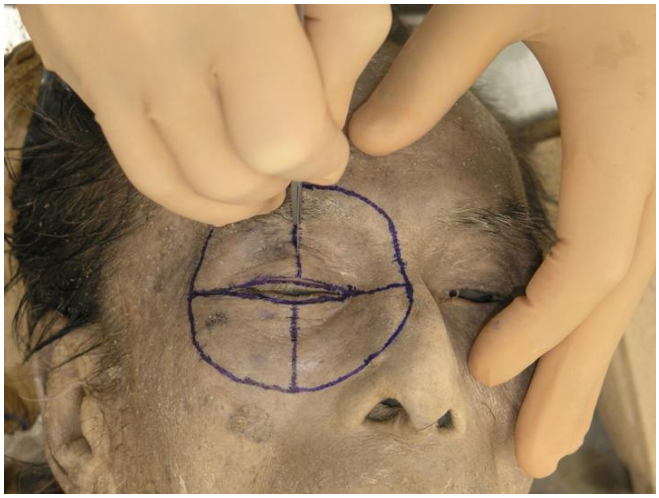

Fig. (1-2). The skin is superficially incised along the marked line.

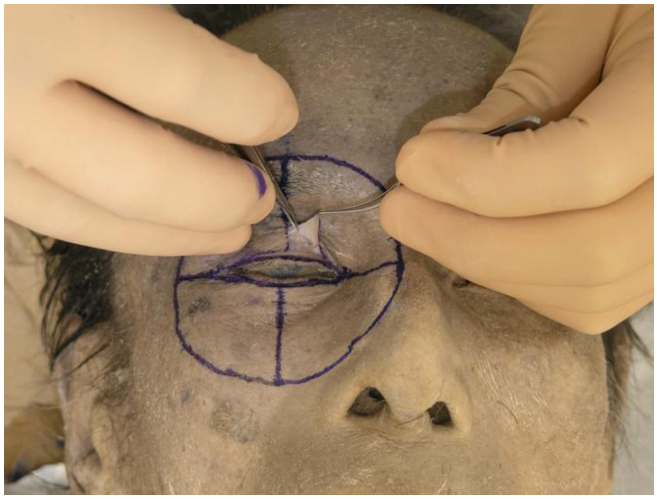

Fig. (1-3). The skin is meticulously detached from the orbicularis oculi muscle (OOM), starting from the eyelid margin.

Tip: As the colour of both the subcutaneous tissue and the OOM is similarly whitish in cadavers, inadvertent dissection makes it impossible to appropriately detach the two layers. As the tissues of cadavers are not as resistant to manipulation as live tissues are, we must discern the difference of each tissue. The subcutaneous tissue of the eyelid is areolar or cotton-like in appearance, and should be left attached to the OOM side during dissection to enable appropriate exposure of the OOM. The subcutaneous tissue on the OOM will be removed later in the dissection process.

C. As the subcutaneous tissue near the dissection borders is very thick, the dissection is performed using ophthalmic scissors or a blade (Fig. **1-4**).

D. Next, the subcutaneous tissue on the OOM is removed. As the anatomy of the OOM, especially around the medial and lateral canthi, should be preserved to allow a detailed analysis, these areas are dissected very meticulously.

Tip: As the subcutaneous tissue of eyelid is very thin, careful dissection is required. First, Westcott scissors are used to open a small hole in the subcutaneous tissue, followed by blunt dissection in the space between the subcutaneous tissue and the OOM. The subcutaneous tissue is removed in pieces.

Fig. (1-4). The dissection near the outer borders is performed using ophthalmic scissors or a blade.

E. After the above steps, the OOM is exposed sufficiently (Fig. **1-5**).

Fig. (1-5). The OOM is sufficiently exposed.

The following structures can then be identified.

a: In the medial canthus, the medial canthal tendon (MCT) continues from the pretarsal OOM [1]. The lower border of the MCT is distinctly linear and the lower preseptal and orbital OOMs attach to the lower border of the MCT or go under the MCT to constitute the posterior lamella of the anterior limb of the MCT. When the lower border of the MCT is incised, it is realized that the preseptal and orbital OOMs go under the MCT. The so-called "MCT" is actually the anterior lamella of the anterior limb of the MCT[1], that is to say, the MCT is a double lamella structure [1]. On the other hand, the upper border of the MCT is usually fluffy and some preseptal and orbital OOMs originate from it [2]. Muscle fibres are usually seen in front of the MCT, which is

part of the corrugator supercilli muscle or the levator labii superioris alaeque nasi.

b: In the lateral canthus, a lateral palpebral raphe is not identified [3, 4]. The lateral palpebral raphe is defined as a narrow fibrous band in the lateral part of the OOM formed by the interlacing of fibres passing through the upper and lower eyelids [5]. Traditionally, it has been thought to be the common tendon of the septal and orbital parts of the OOM [6], or the linear tendon of these parts attaching to the zygomatic bone [7]. In contrast, there are also reports refuting the presence of the raphe, suggesting that the OOM in the lateral part is continuous without tendinous intercalation [3, 8].

2. DISSECTION OF THE UPPER EYELID

A. The periosteum of the upper half of the orbital rim is first incised with a blade (Fig. **2-1**).

Fig. (2-1). The periosteum of the upper half of the orbital rim is incised with a blade.

The medial and lateral canthi remain intact (the inferior extents of this incision is approximately 1 cm above the MCT and the lateral canthal band (LCB) [9]).

Detailed Anatomy: The LCB is a composite structure of the tendinous and ligamentous components in the lateral canthus, which were formerly called the "lateral canthal tendon (LCT)" or the "lateral canthal ligament (LCL)" [9].

B. The periosteum is detached from the frontal bone with an elevator to the arcus marginalis [10]. The superior orbital notch or foramen, through which the superior orbital nerve passes, can be identified (Fig. **2-2**).

Detailed Anatomy: The arcus marginalis is the junction between the orbital septum, periosteum and periorbita, in particular the angular part between the orbital septum and the periorbita [10].

C. Next, Westcott scissors are used to completely incise the periosteum until the orbital fat is seen (Fig. **2-3**).

D. The detached orbicularis-periosteum complex is then reflected inferiorly (Fig. **2-4**).

The preaponeurotic fat pad and the medial fat pad can be identified at this stage [10], although this photograph does not show them because of the small volume of fat.

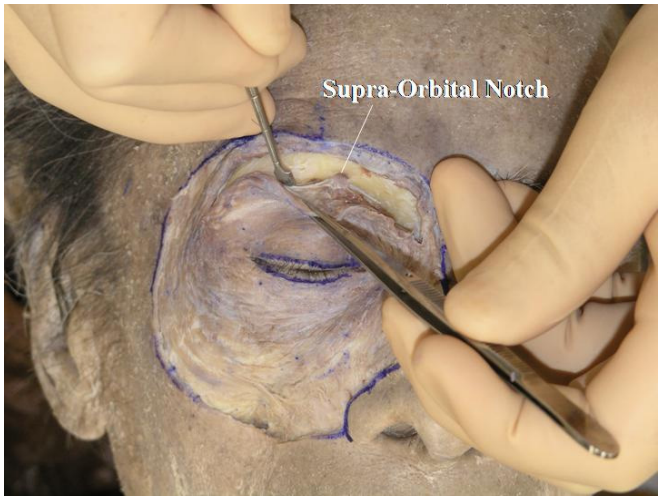

Fig. (2-2). The periosteum is detached from the frontal bone to the arcus marginalis.

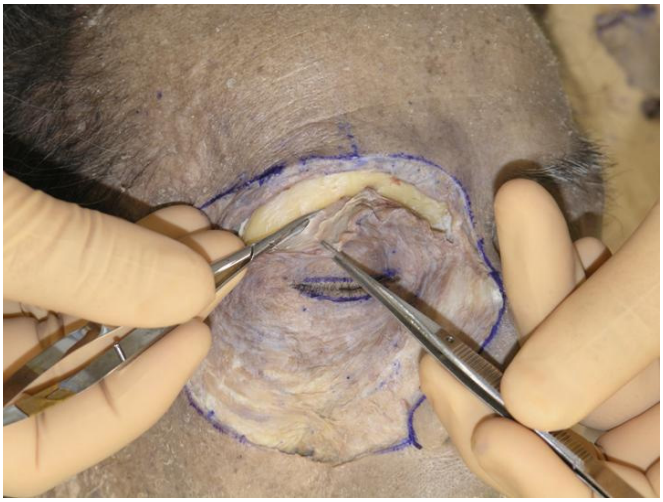

Fig. (2-3). The periosteum is incised until the orbital fat can be visualized.

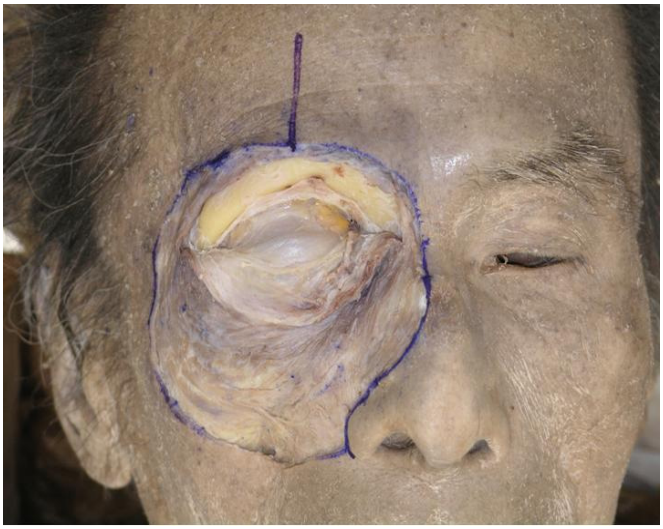

Fig. (2-4). The detached orbicularis-periosteum complex is reflected inferiorly.

Tip: All cotton-like tissues should to be attached to the inferiorly reflected complex to allow a better visualization of the ligaments attaching to the orbital septum.

E. At this stage it is still difficult to identify the course of the levator palpebrae superioris (LPS) muscle, therefore part of the frontal bone should be removed. First, a vertical line is drawn from the centre of the orbital rim (Fig. **2-4**) and then the periosteum is detached (Fig. **2-5**).

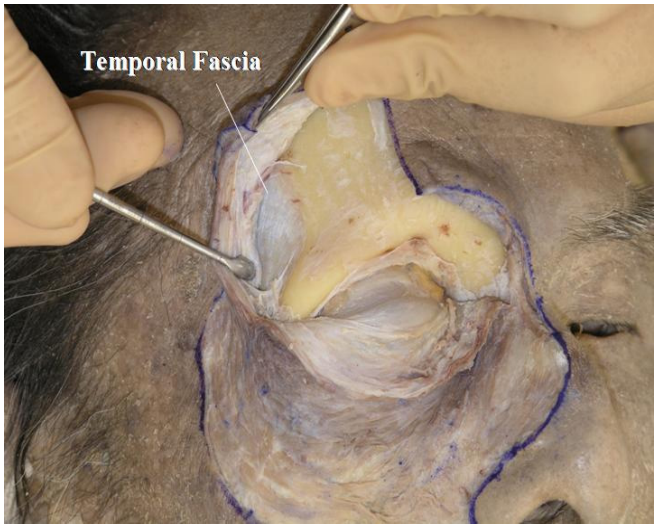

Fig. (2-5). The periosteum is maximally detached. The temporal fascia is shown laterally to originate from the frontal bone-like periosteum.

The temporalis fascia is observed laterally, originating from the frontal bone-like periosteum (Fig. **2-5**).

F. After detaching the periosteum from the frontal bone, the bone is exposed sufficiently using three traction sutures (Fig. **2-6**), which are fixed to the skin.

Fig. (2-6). The bone is exposed using three traction sutures.

G. Detaching the periorbita of the superior orbital wall allows removal of part of the frontal bone including the superior orbital rim using a chisel and a hammer. This enables identification of the LPS muscle and its surrounding structures (Figs. **2-7, 2-8**).

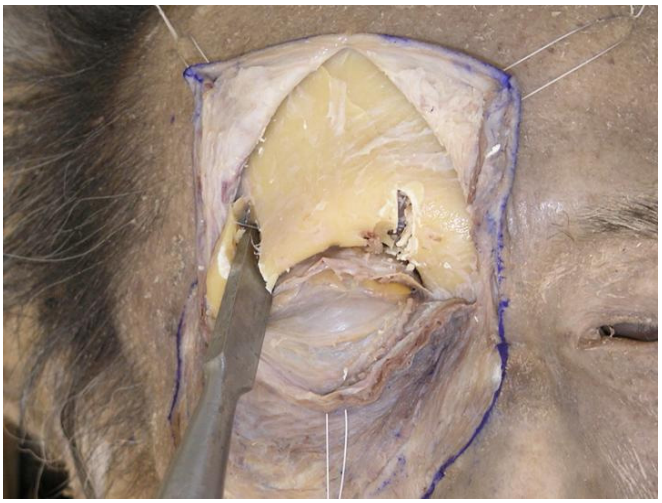

Fig. (2-7). Part of the frontal bone, including the superior orbital rim, is removed.

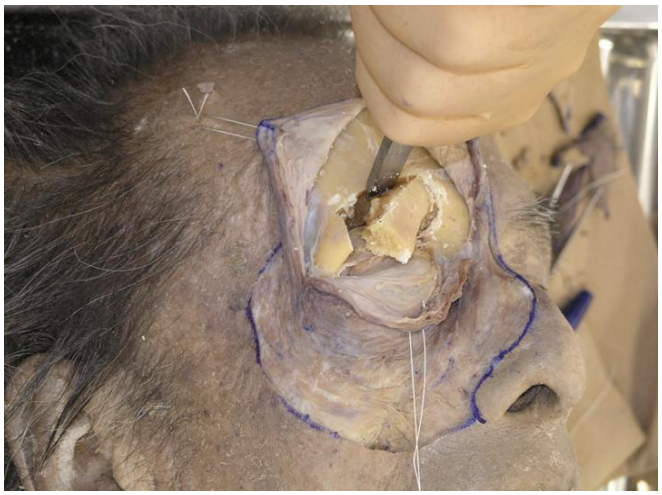

Fig. (2-8). Same explanation as above.

The medial edge is adjacent to the lateral side of the trochlea and the lateral edge is at the lateral border of the superior orbital rim.

H. When the bone is removed, the periorbit can be seen (Fig. **2-9**), and it is then incised vertically (Fig. **2-10**).

Fig. (2-9). The periorbit still remains after bone removal.

Fig. (2-10). The periorbit is incised vertically and the bone is further removed.

If the working field is too small, the bone can further be removed (Fig. **2-10**).

I. The periorbit is then completely removed and the orbital fat can clearly be seen (Fig. **2-11**).

Fig. (2-11). The periorbit is removed completely and the orbital fat can be easily visualized.

J. The orbital fat is carefully removed to expose the LPS muscle and its surrounding structures (Fig. **2-12**).

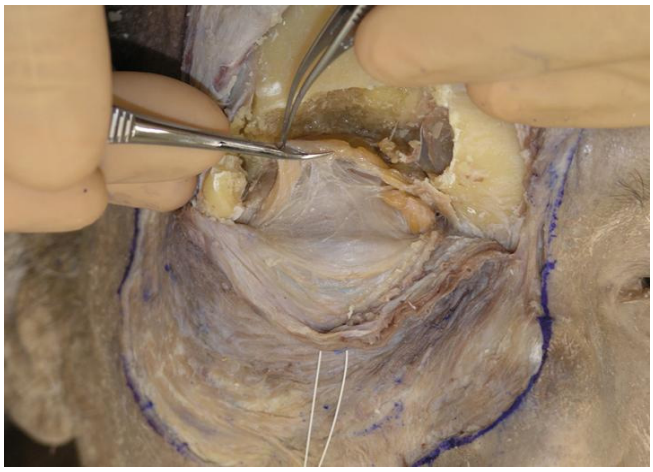

Fig. (2-12). The orbital fat is carefully removed.

Tip: All the cotton-like tissues should be detached from the orbital fat. Certain ligamentous structures may be difficult to discern from the cotton-like structures.

K. The anterior part of the LPS muscle and its surrounding structures behind the orbital septum are exposed (Fig. **2-13**).

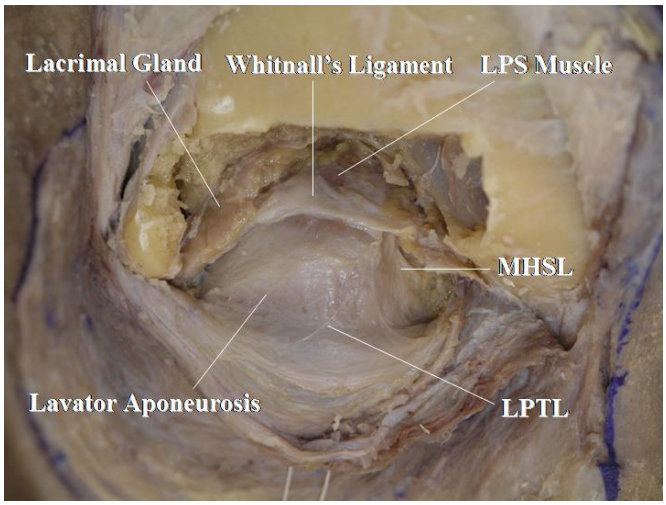

Fig. (2-13). The anterior part of the levator palpebrae superioris (LPS) muscle and its surrounding structures behind the orbital septum are exposed. LPTL: lower positioned transverse ligament, MHSL: medial horn supporting ligament.

The LPS muscle, Whitnall's ligament, lower positioned transverse ligament (LPTL) [11-14], medial horn supporting ligament (MHSL) [15], lacrimal gland and the continuation of the levator aponeurosis to the orbital septum are identified [16].

Detailed Anatomy: Whitnall's ligament is always located on the LPS muscle but the LPTL is always located on the levator aponeurosis [10]. Ligaments supporting the orbital septum are sometimes seen [17].

Detailed Anatomy: Whitnall's ligament connects the lateral aspect of the trochlea and the shallow part of the lateral orbital wall (Whitnall's tubercle) [18]. It acts as a pulley of the LPS muscle cooperating with the intermuscular transverse ligament (ITL) [19-21]. In the lateral area, Whitnall's ligament passes between the orbital and palpebral lobe of the lacrimal gland.

Detailed Anatomy: Whitnall's tubercle [18] is a small protuberance of the zygomatic bone, just within the lateral orbital margin at its centre and about 2 mm below the frontozygomatic suture. It was originally called the "orbital tubercle". It is important as a marking point of attachment of the lateral check ligament, the lateral canthal band, lateral horn of the levator aponeurosis, as well as the ITL, Whitnall's ligament, LPTL and Lockwood's ligament [22] in the lower eyelid. Lockwood's ligament is described later.

Detailed Anatomy: The ITL is the counterpart of Whitnall's ligament, located between the LPS muscle and the superior rectus muscle [19-21]. The ITL connects the trochlea and Whitnall's tubercle [18]. In the lateral area, the ITL supports the palpebral lobe of the lacrimal gland from behind [21].

Detailed Anatomy: The LPTL connects the anterior surface of the trochlea and Whitnall's tubercle [13]. On the lateral half, it supports the orbital septum. The role of the LPTL is to support the preaponeurotic fat pad [14].

Detailed Anatomy: The MHSL connects the trochlea, Whitnall's ligament, medial horn of the levator aponeurosis and medial orbital rim [15]. The MHSL tightly attaches to the medial horn, but is loosened by involutional changes. The MHSL can be a mark of the medial border of the levator aponeurosis.

L. Next, the orbicularis-septum complex is incised vertically at the central part of the upper eyelid, and the confluent part of the orbital septum and levator aponeurosis can be identified from the front and the back (Fig. **2-14**).

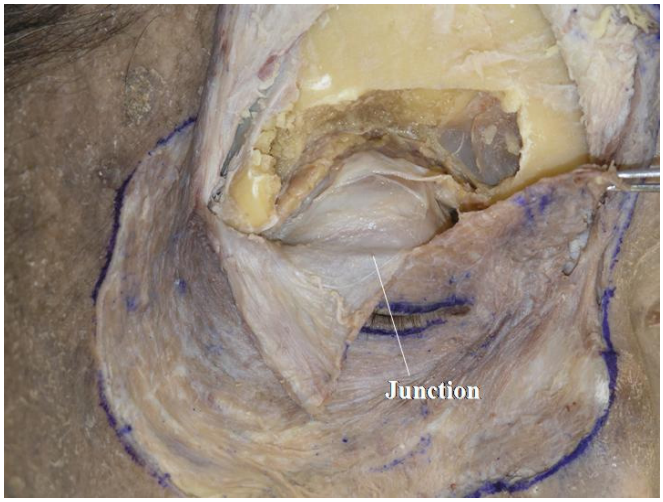

Fig. (2-14). The confluent point of the orbital septum and levator aponeurosis is shown.

Detailed Anatomy: The confluent part is always situated above the superior border of the tarsal plate in Asians, as well as in Caucasians [16]. However, in the lateral part, some cases may show the junction on the tarsal plate [16].

M. The confluent part is then incised horizontally and the orbicularis-septum complex is pulled aside. Here, the medial and lateral canthal regions are kept intact (Fig. **2-15**).

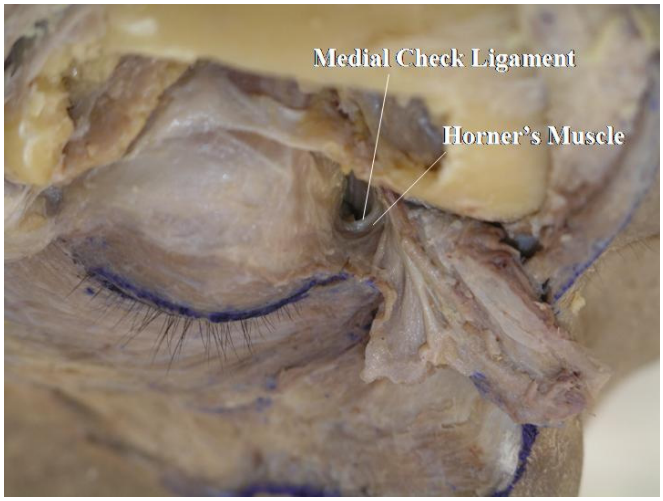

Fig. (2-15). The confluent part is incised horizontally and the orbicularis-septum complex is pulled aside.

If the orbital fat around the medial canthus is removed, the origin of Horner's muscle and the medial check ligament are seen.

Detailed Anatomy: Horner's muscle is part of the OOM, specifically located around the medial canthal region. Horner's muscle supports the medial aspect of the tarsal plate, together with the medial rectus capsulopalpebral fascia (mrCPF) (described later) [23]. In addition, Horner's muscle is the main power source of the lacrimal drainage system [24].

Detailed Anatomy: The medial check ligament connects the medial rectus muscle pulley and the medial orbital wall, passing behind Horner's muscle. The medial check ligament is part of the mrCPF [23] and regulates the position of the medial rectus muscle pulley.

N. Bone is further removed to allow better visualization of the lateral canthal area (Fig. **2-16**).

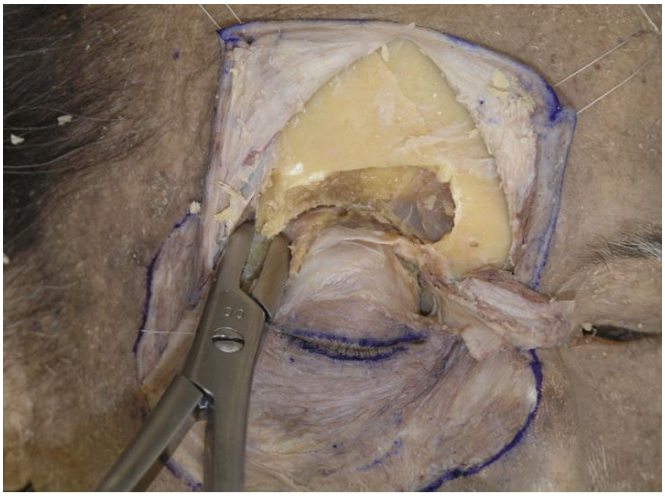

Fig. (2-16). The bone is further removed to visualize the lateral canthal area.

O. Here we can identify the thin medial horn and the robust lateral horn of the levator aponeurosis, the course of the Whitnall's ligament and the MHSL and the orbital lobe of the lacrimal gland (Fig. **2-17**).

Fig. (2-17). The thin medial horn and the robust lateral horn of the levator aponeurosis, Whitnall's ligament, medial horn supporting

ligament (MHSL) and the orbital lobe of the lacrimal gland are shown, although in this figure, the MHSL is not demonstrated (See Fig. **2-13**).

Detailed Anatomy & Clinical Hint: The orbital lobe of the lacrimal gland is located more anteriorly than the palpebral lobe. Lacrimal gland protrusion through the conjunctiva is caused by prolapse of the palpebral lobe.

P. The OOM in the upper eyelid margin is then carefully detached from the levator aponeurosis (Fig. **2-18**).

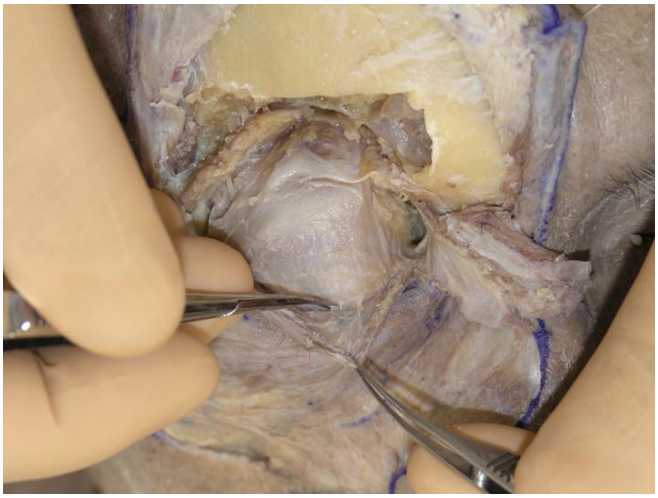

Fig. (2-18). The orbicularis oculi muscle in the upper eyelid margin is carefully detached from the levator aponeurosis.

Q. The levator aponeurosis reaches the area around the eyelid ciliary roots (Fig. **2-19**).

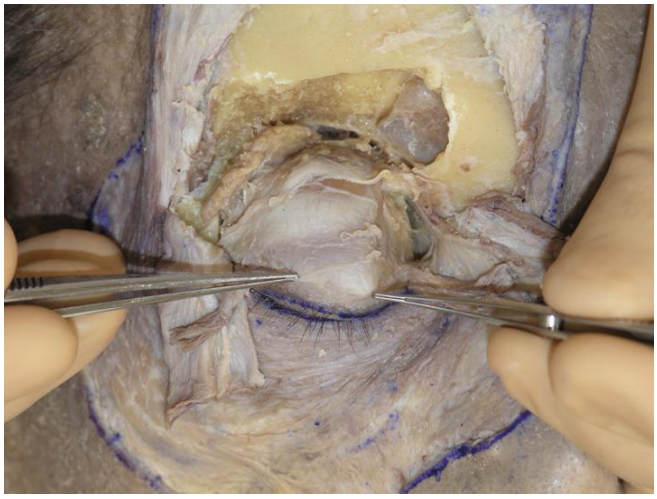

Fig. (2-19). The levator aponeurosis is seen to reach the ciliary roots.

R. Further dissection can allow a better visualization of the relationship between the levator aponeurosis and the ciliary roots (Fig. **2-20**).

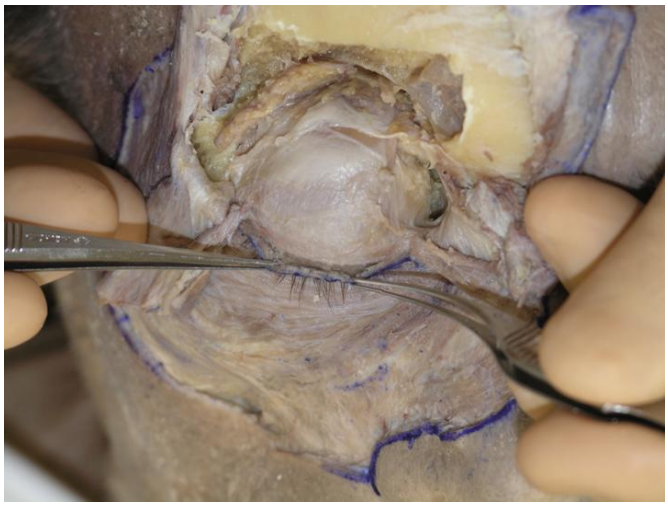

Fig. (2-20). The relationship between the levator aponeurosis and the ciliary roots is shown.

When dissecting around the ciliary roots, a hard fibrous tissue is felt, that is to say, cilia grow from a robust fibrous tissue.

Clinical Hint: The findings indicate that it is hard to infiltrate local aniesthesia directly to the ciliary area.

S. The insertion of Müller's muscle is incised to expose the upper border of the tarsal plate (Fig. **2-21**).

Detailed Anatomy: Although there are some Müller's muscles in the eyelid and the orbit, namely in the upper eyelid, the lower eyelid and the orbital apex, the term "Müller's muscle" used in this article mean the upper eyelid Müller's muscle.

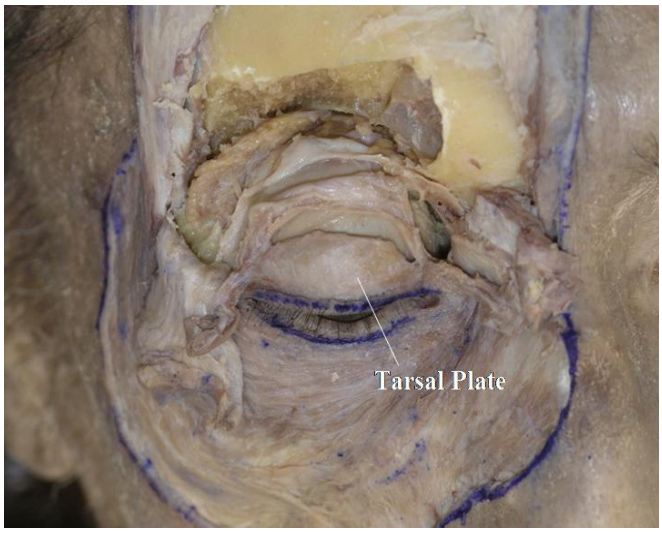

Fig. (2-21). The shape of the upper tarsal plate tapers medially.

The shape of the tarsal plate can now be analysed. In general, it tapers to a greater extent medially.

T. The space between the levator aponeurosis and the Müller's muscle (post-aponeurotic space) is exposed (Fig. **2-22**).

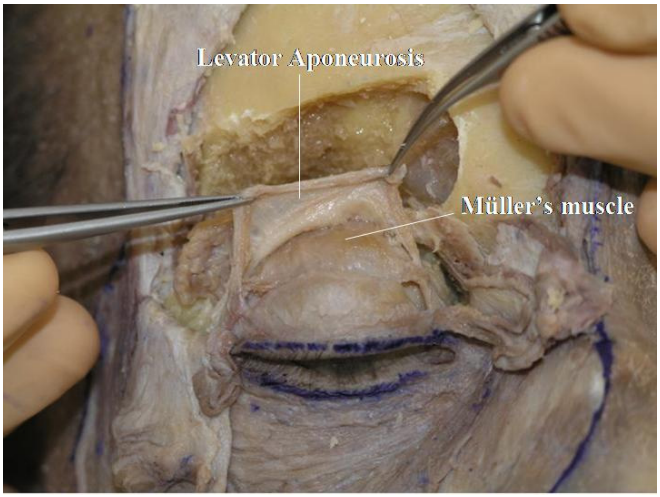

Fig. (2-22). The space between the levator aponeurosis and Müller's muscle is exposed.

This dissection is easily performed. The dissection can be quicker if Müller's muscle is pulled downward during the dissection.

U. Müller's muscle is detached from the conjunctiva (Fig. **2-23**).

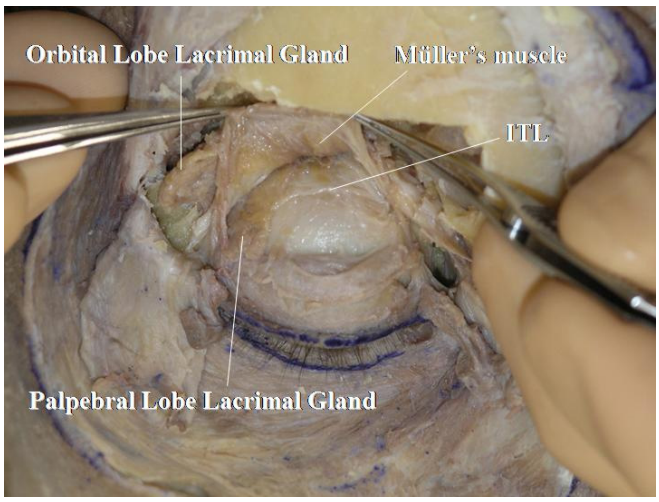

Fig. (2-23). The intermuscular transverse ligament (ITL) is shown to pass under the palpebral lobe of the lacrimal gland.

The ITL can be visualized passing under the palpebral lobe of the lacrimal gland.

V. The ITL reaches the lateral orbital wall (Whitnall's tubercle) (Fig. **2-24**).

W. After confirming the location of Whitnall's ligament from the front (Fig. **2-25**), the levator aponeurosis and Müller's muscle are incised vertically.

The ITL and Whitnall's ligament are shown to oppose the LPS muscle from both sides (Fig. **2-26**).

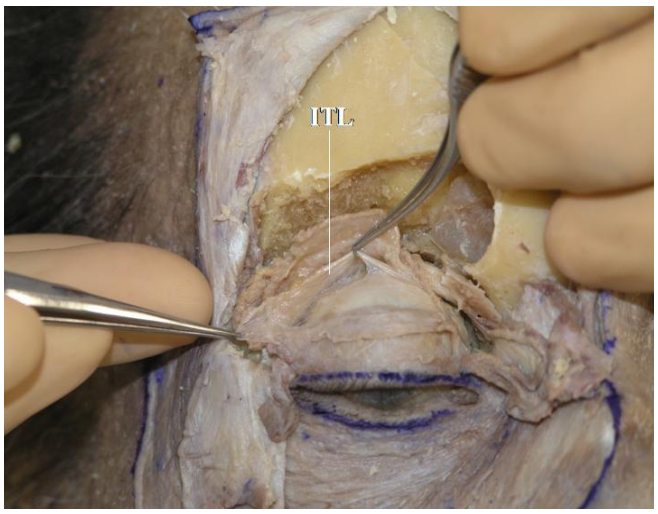

Fig. (2-24). The ITL reaches the lateral orbital wall (Whitnall's tubercle).

Fig. (2-25). Whitnall's ligament is again visualized.

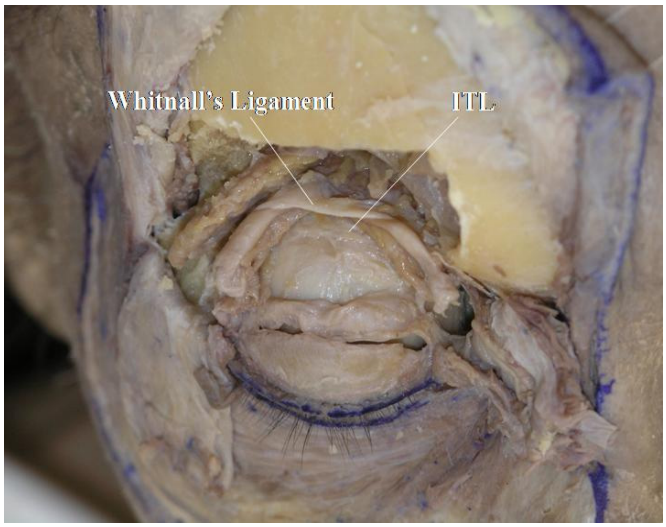

Fig. (2-26). The ITL and Whitnall's ligament are shown to oppose the LPS muscle from both sides.

3. Dissection of the Lower Eyelid

A. The periosteum of the lower half of the orbital rim is incised with a blade (Fig. **3-1**).

Fig. (3-1). The periosteum of the lower half of the orbital rim is incised with a blade.

The medial and lateral canthal areas remain intact (up to one cm below the MCT or the LCB).

B. The periosteum is then detached from the bone using an elevator up to the arcus marginalis [25] (Fig. **3-2**).

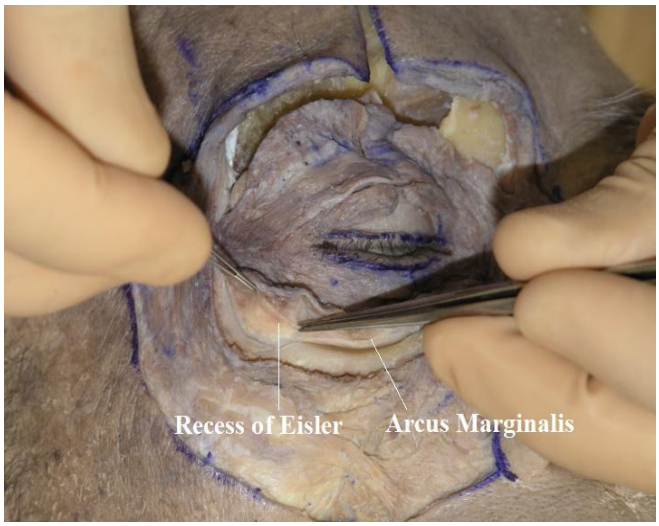

Fig. (3-2). The periosteum is detached from the bone up to the arcus marginalis. The "recess of Eisler" is shown in the lateral part.

In the lateral part, the orbital septum attaches to the inferior orbital rim and lightly beyond it, in an area called the "recess of Eisler" [26].

C. Next, Westcott scissors are used to incise the periosteum until the orbital fat is visualized (Fig. **3-3**).

D. While dissecting under the OOM inferolaterally, a thick fibrous structure is encountered (Fig. **3-4**).

This fibrous structure, which supports the OOM from behind, is called the "orbitomalar ligament" [27]. This structure is also called the "orbicularis retaining ligament" by the plastic surgeons [28].

Fig. (3-3). The periosteum is incised until the orbital fat is visualized.

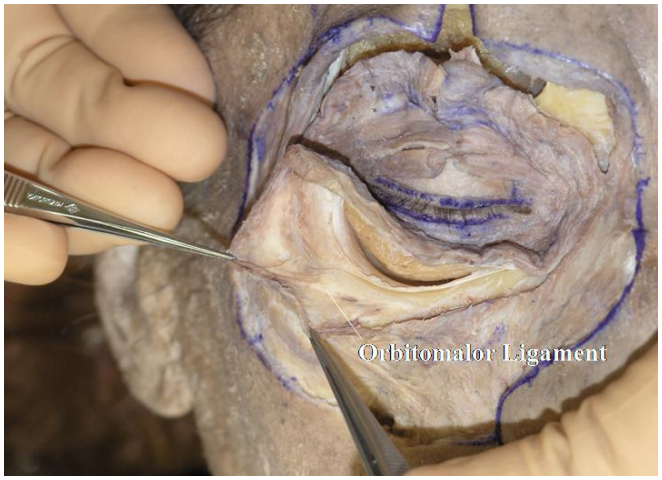

Fig. (3-4). A thick fibrous structure, called the "orbitomalor ligament", is encountered on the Zygomatic bone.

Tip: The "orbitomalar ligament" term was first used by Kikkawa *et al*., before using the term "orbicularis retaining ligament".

E. The detached orbicularis-periosteum complex is then reflected superiorly (Fig. **3-5**).

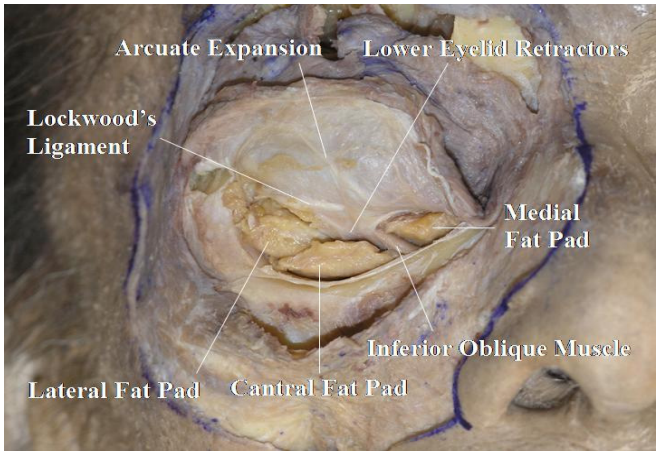

Fig. (3-5). The confluent part between the lower eyelid retractors (LERs) and the orbital septum is shown. The orbital fat is divided into three compartments: medial, central and lateral.

The confluent part between the lower eyelid retractors (LERs) and the orbital septum is seen here. Careful removal of the orbital fat, shows that it is divided into three parts: medial, central and lateral [25].

Tip: All the cotton-like tissues should to be attached to the reflected tissue to allow a better visualization of the ligaments attaching to the orbital septum.

Detailed Anatomy: The medial and central fat compartments are divided by the inferior oblique muscle, and the central and lateral compartments are divided by the arcuate expansion of Lockwood's ligament [25].

Detailed Anatomy: The arcuate expansion of Lockwood's ligament, which originates from the posterior lacrimal crest, attaches to the orbital septum [29]. Some other supporting ligaments may be observed on the orbital septum [17]. Dissection of the arcuate expansion is performed later.

Detailed Anatomy: The LERs are constituted by the capsulopalpebral head (CPH), CPF and smooth muscle fibres [25, 30]. The CPH originates from the inferior rectus fascia, goes forward, surrounds the inferior oblique muscle and reaches Lockwood's ligament. It then becomes the CPF. The CPF originates from Lockwood's ligament and reaches the inferior border of the tarsal plate and the subcutaneous tissue through the OOM. Passing around the inferior conjunctival fornix, the CPF includes a large number of smooth muscle fibres.

F. After dissecting the area under the OOM, the levator labii superioris muscle can be visualized. After incising the origin of the lavator labii superioris muscle and reflecting it downward, the infraorbital nerve is seen rising from the infraorbital foramen (Fig. **3-6**).

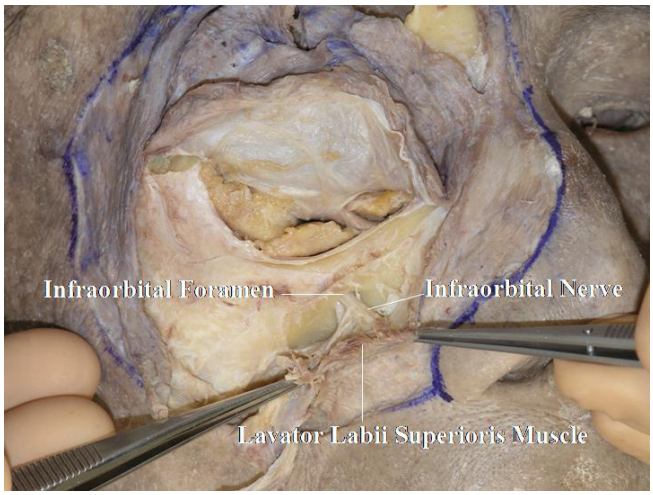

Fig. (3-6). The infraorbital nerve is seen arising from the infraorbital foramen.

Detailed Anatomy: The position of the infraorbital foramen is generally around 25 to 28 mm from the central facial line and 6 to 9 mm from the inferior orbital rim [31].

G. At this stage, part of the bone should be removed to allow better visualization of the LERs and their related structures. Initially, a large area of the periosteum on the bone and the periorbit on the orbital floor are detached (Fig. **3-7**).

Fig. (3-7). A large area of the periosteum on the bone and the periorbit on the orbital floor are detached.

H. The bone, including the inferior orbital rim, is removed using a chisel and a hammer (Fig. **3-8**).

Fig. (3-8). The bone, including the inferior orbital rim, is removed.

The medial edge of the removed bone does not involve the origin of the inferior oblique muscle. The lateral edge reaches the lateral border of the inferior orbital rim.

I. The bone is usually removed together with the floor, and the orbital contents are then seen to be supported by the periorbita. The oblique course of the infraorbital nerve can be visualized (Fig. **3-9**).

The infraorbital nerve arises from the superolateral posterior corner of the maxillary sinus roof. The space around the nerve is narrow.

J. After removal of the infraorbital nerve, the hiatus maxillaris is seen at the medial upper part of the maxillary sinus (Fig. **3-10**).

K. The reflected orbicularis-septum complex is pulled superiorly with a suture and the periorbit of the floor is removed (Fig. **3-11**).

Although the fat of the lower eyelid is divided into 3 compartments, they all originate from the fat in the deeper orbit [25].

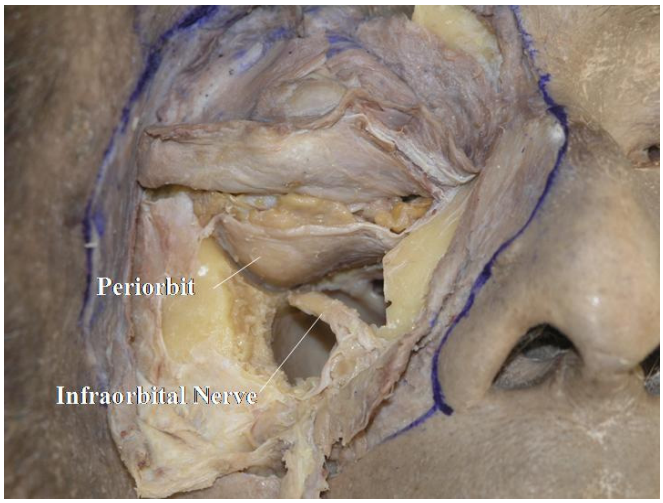

Fig. (3-9). The oblique course of the infraorbital nerve can be visualized.

Fig. (3-10). The hiatus maxillaris is seen at the medial upper part of the maxillary sinus.

Fig. (3-11). The fat compartments of the lower eyelid originally derive from the same fat in the deeper orbit.

L. The orbital fat is then maximally removed, surpassing the medial and lateral recti muscles (Fig. **3-12**).

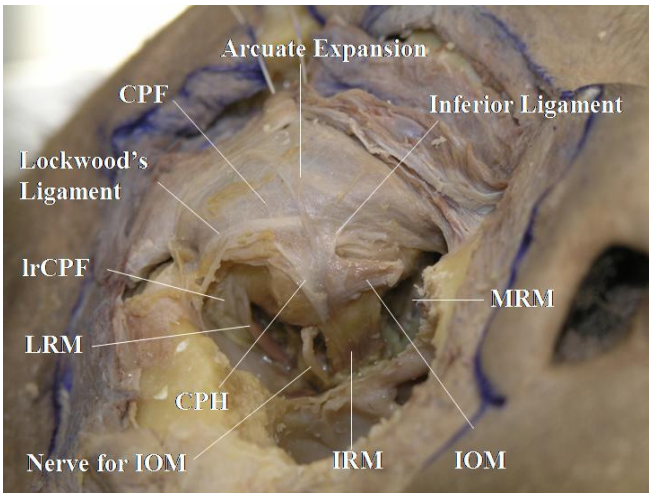

Fig. (3-12). The inferior rectus muscle, inferior oblique muscle and its nerve, the LERs and the medial and lateral recti muscles and their check ligaments (including the medial rectus CPF (mrCPF) and lateral rectus CPF (lrCPF) are visualized. The medial rectus CPF is obscure in this figure. LRM: lateral rectus muscle, CPH: capsulopalpebral head, IOM: inferior oblique muscle, IRM: inferior rectus muscle, MRM: medial rectus muscle.

To allow an easier removal of the fat, the inferior oblique muscle tendon may be incised. Here, the inferior rectus muscle, inferior oblique muscle and its nerve, the LERs and the medial and lateral recti muscles and their check ligaments (including the medial rectus CPF (mrCPF) and lateral rectus CPF (lrCPF)) [23, 32] are visualized.

M. When the incised inferior oblique tendon is pulled laterally, the origin of Lockwood's ligament and its colleague ligaments are visualized at the posterior lacrimal crest (Fig. **3-13**).

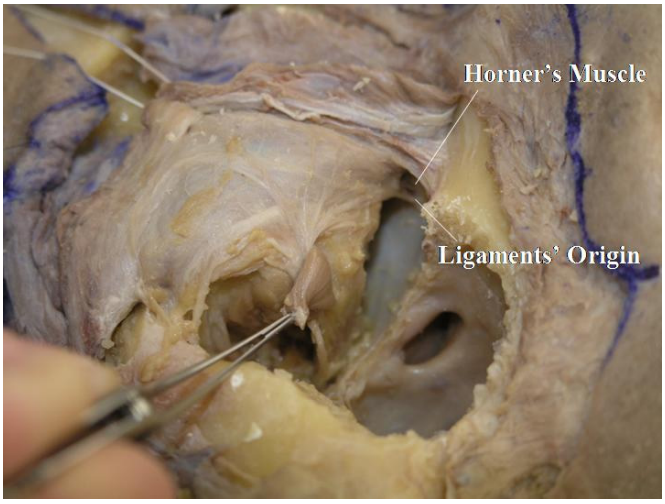

Fig. (3-13). The origin of Lockwood's ligament and its colleague ligaments are visualized at the posterior lacrimal crest.

In addition, a fibrous tissue connecting the medial rectus muscle fascia with the eyelid can be seen. This is called the "mrCPF" [23]. In the lateral canthus, the fibres connecting the lateral rectus muscle fascia to the eyelid are called the "lrCPF" [32].

Detailed Anatomy: The lower eyelid is supported by 3 ligaments: the arcuate expansion of Lockwood's ligament,

Lockwood's ligament, and the inferior ligament [29]. The ligaments originate from the posterior lacrimal crest. The arcuate expansion, corresponding to the LPTL in the upper eyelid, takes its course around the confluent part between the orbital septum and the LERs, and inserts onto the inferolateral orbital rim. Lockwood's ligament, corresponding to Whitnall's ligament in the upper eyelid, inserts onto Whitnall's tubercle in the lateral canthus and becomes part of the lateral retinaculum (which is explained later). The inferior ligament, corresponding to the MHSL, supports the medial aspect of the LERs.

Detailed Anatomy: In the medial canthus, the mrCPF supports the medial aspect of the tarsal plate together with Horner's muscle [23]. Therefore, the medial aspect of the tarsal plate is not supported by the so-called "MCT" or the "MCL". The mrCPF contains the medial rectus muscle pulley, medial check ligament and many smooth muscle fibres. It enables a synchronous movement of the eyelid and the globe [23, 33]. The mrCPF sends fibres to the caruncle as well.

Detailed Anatomy: In the lateral canthus, the lrCPF supports the lateral aspect of the tarsal plate together with the LCB [32]. The lrCPF contains the lateral rectus muscle pulley, lateral check ligament, and a small amount of smooth muscle fibres. It enables a synchronous movement of the eyelid and the globe [32, 33]. As the lrCPF receives some muscle fibres from the muscle of Riolan, the lrCPF acts also as an intermediate tendon [32].

Detailed Anatomy: The "Muscle of Riolan" is part of the OOM, situated in the eyelid margin, around the ciliary roots [34]. It is divided into 3 parts: pars ciliaris, pars fascicularis and pars subtarsalis. Pars ciliaris is situated on the tarsal plate, pars subtarsalis is located under the Meibomian ducts and pars fascicularis connects pars ciliaris with pars subtarsalis.

N. The traction suture of the orbicularis-septum complex is loosened and the centre of the complex is incised vertically (Fig. **3-14**).

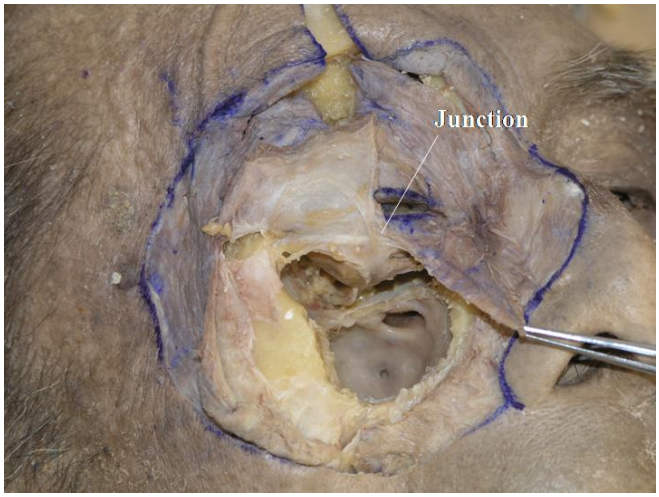

Fig. (3-14). The junction between the orbital septum and the LERs is visualized.

The junction between the orbital septum and the LERs is visualized. It is located around the point surpassing Lockwood's ligament [35, 36] but is always situated below the lower border of the tarsal plate [35].

O. The orbicularis-septum complex is incised at the junction of the orbital septum and the LERs but the medial and lateral canthal areas are kept intact (Fig. **3-15**).

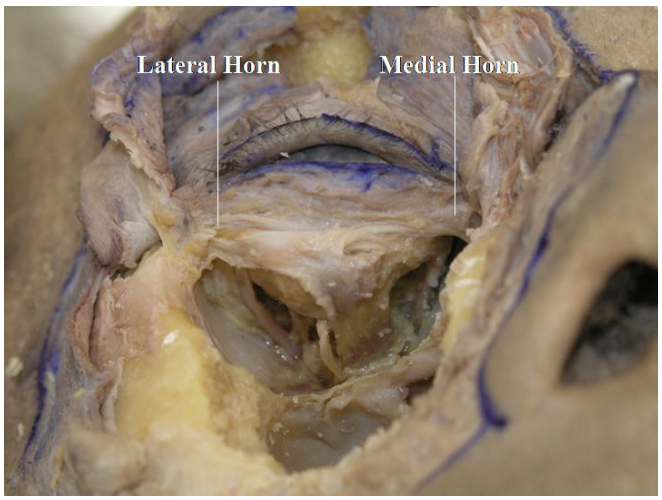

Fig. (3-15). The thin medial horn and the thick lateral horn of the LERs can be seen.

The thin medial horn and the thick lateral horn of the LERs can be seen [37].

P. Next, the pretarsal OOM is removed (Fig. **3-16**)

Fig. (3-16). The pretarsal OOM is removed.

The insertion of the LERs to the lower border of the tarsal plate is visualized (Fig. **3-17**).

The ciliary roots are seen here growing on the tarsal plate. Some LERs' fibres appear to cover the anterior surface of the tarsal plate, which is the anterior layer of the LERs.

Detailed Anatomy: The LERs are constituted by double layers [38, 39]. The posterior layer is the main tractional component, which includes any smooth muscle fibres and reaches the inferior border of the tarsal plate. The anterior layer originates from Lockwood's ligament and on its way merges with the suborbicularis fascial tissue and the orbital septum, and reaches the subcutaneous tissue through the OOM.

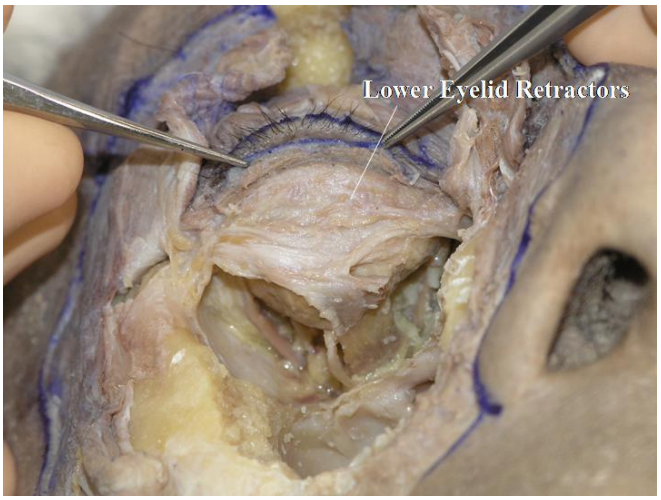

Fig. (3-17). The insertion of the LERs to the lower border of the tarsal plate is visualized. The ciliary roots can be seen growing on the tarsal plate.

Q. Insertion of the LERs is incised to expose the lower border of the tarsal plate (Fig. **3-18**).

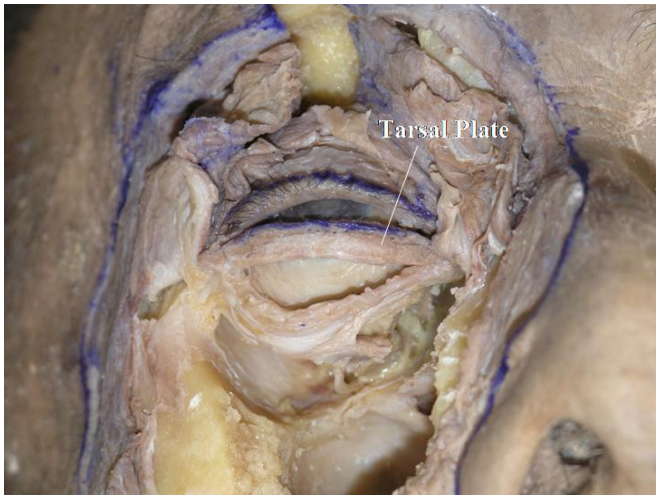

Fig. (3-18). The lower tarsal plate is exposed. Its shape is usually rectangular.

The shape of the tarsal plate can be seen. The lower tarsal shape is usually rectangular, meaning that the lower border is parallel to the eyelid margin.

4. Dissections of the Conjunctival Fornix, Extraocular Muscle Insertions, and Medial and Lateral Canthi

A. The relationship between the pretarsal OOM and the MCT is analysed again. These structures are continuous but it may be lightly obscure in this specimen (Fig. **4-1**).

Detailed Anatomy: The OOM is divided into 3 parts: pretarsal, preseptal and orbital. The orbital part is situated on the bone and not on the orbital septum.

B. The muscle fibers running in front of the MCT are removed, and this enables a better understanding of the relationship between the OOM and the MCT (Fig. **4-2**).

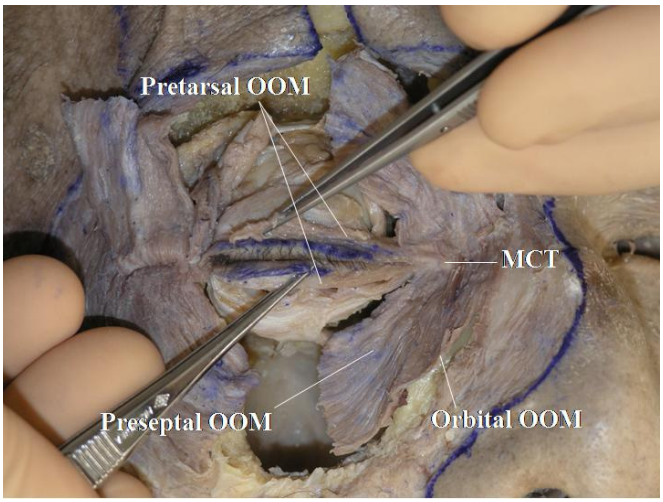

Fig. (4-1). The pretarsal orbicularis oculi muscle (OOM) is continuous with the medial canthal tendon (MCT).

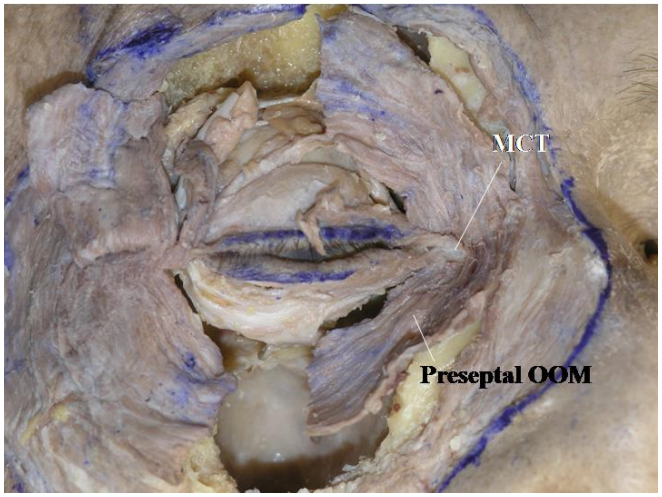

Fig. (4-2). The muscles fibers running in front of the MCT are removed.

The branched-out tendon may be seen from the superior side of the MCT. On the other hand, the preseptal and orbital OOM fibres are seen passing under the medial canthal tendon.

Detailed Anatomy: Muscle fibres running in front of the MCT are part of the corrugator supercilli muscle or the levator labii superioris alaeque nasi.

C. The upper and lower tarsi are then incised vertically at their center and then reflected. In this specimen, the conjunctival fornix forms a circular shape (Fig. **4-3**).

Detailed Anatomy: The conjunctival fornix is round shaped in anatomical dissections, however, in reality, due to the ligamentous supports, the extent of elongation may vary [40]. in the lower eyelid in particular, as Lockwood's ligament and its related ligaments originate from the posterior lacrimal crest and disperse laterally, the lower conjunctival fornix is narrower medially and wider laterally [40].

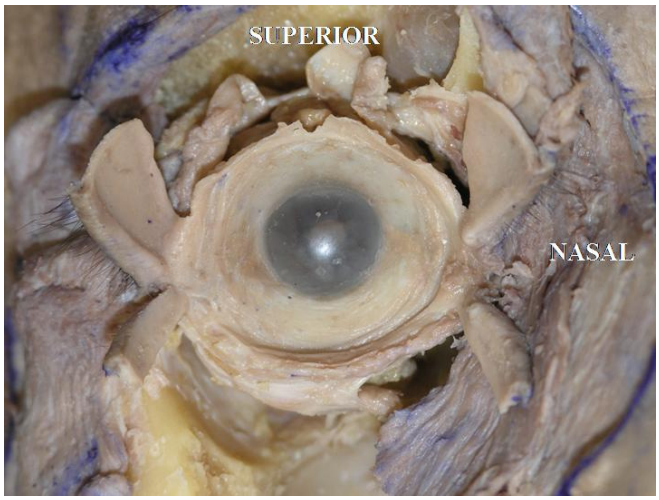

Fig. (4-3). The conjunctival fornix has a round shape.

D. Next, the conjunctiva and Tenon's fascia are removed, allowing visualization of the insertions of the extraocular muscles.

E. The insertion of the medial rectus muscle tendon is usually located 5.5 mm from the medial corneal limbus [18] (Fig. **4-4**).

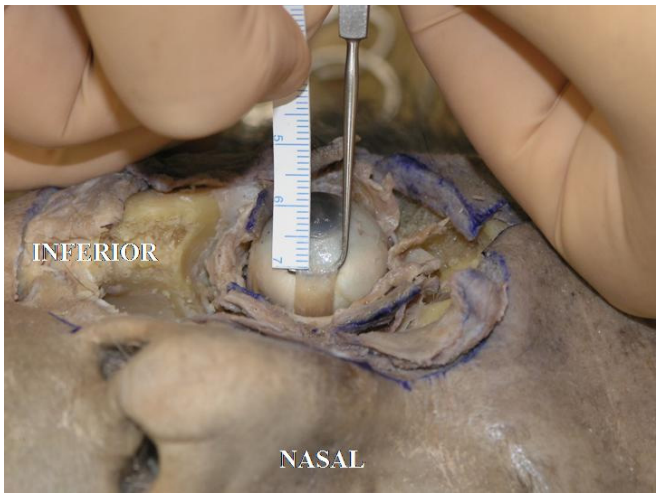

Fig. (4-4). The insertion of the medial rectus muscle tendon is usually located 5.5 mm from the medial corneal limbus

The insertion is almost parallel to the limbus. The width is 5.5mm in this specimen (Fig. **4-5**).

F. The insertion of the inferior rectus muscle tendon is in usually located 6.5 mm from the inferior corneal limbus [18] (Fig. **4-6**).

The insertion is laterally slanted to the limbus. The width is about 6.0 mm in this specimen (Fig. **4-7**).

G. The insertion of the lateral rectus muscle tendon is in usually located 6.9 mm from the lateral corneal limbus [18] (in this specimen it is 6.5 mm) (Fig. **4-8**).

The insertion is almost parallel to the limbus. The width is about 7.0 mm in this specimen (Fig. **4-9**).

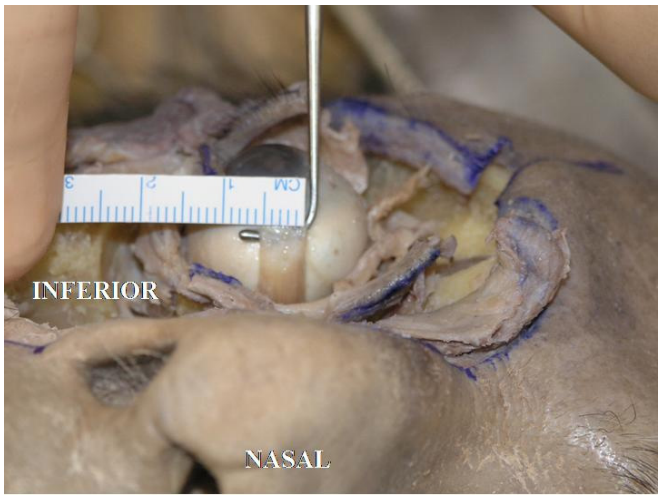

Fig. (4-5). The insertion is almost parallel to the limbus. The width is 5.5mm in this specimen.

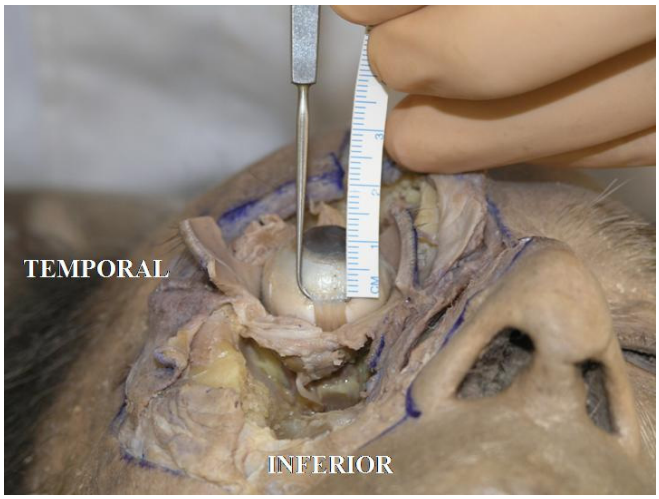

Fig. (4-6). The insertion of the inferior rectus muscle tendon is usually located 6.5 mm from the inferior corneal limbus.

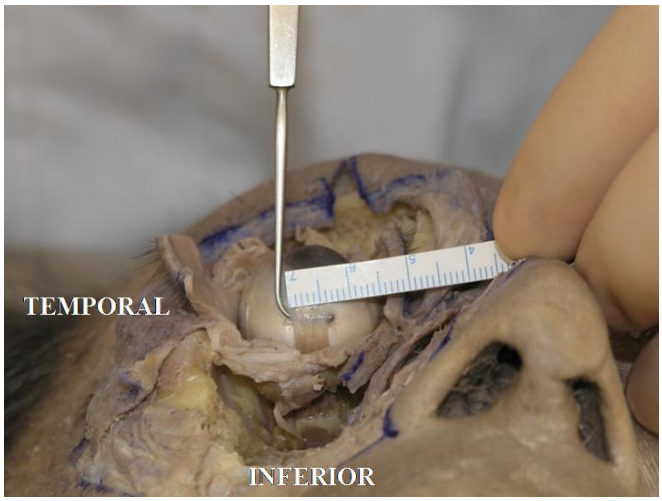

Fig. (4-7). The insertion width of the inferior rectus muscle tendon is laterally slanted to the limbus. The width is about 6.0 mm in this specimen

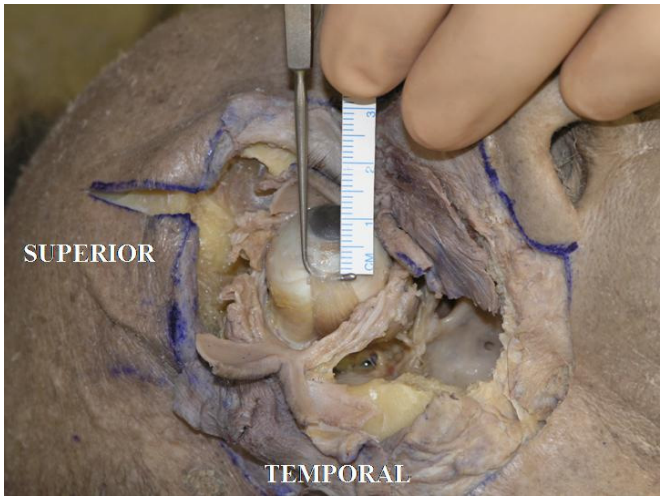

Fig. (4-8). The insertion of the lateral rectus muscle tendon is located 6.5 mm from the lateral corneal limbus.

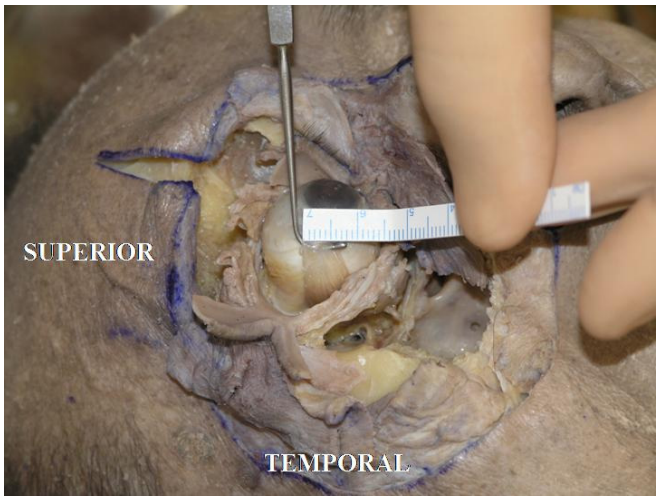

Fig. (4-9). The insertion width of the lateral rectus muscle tendon is almost parallel to the limbus. The width is about 7.0 mm in this specimen.

H. The insertion of the superior rectus muscle tendon is usually located 7.7 mm from the superior corneal limbus [18] (In this specimen it measured 7.5 mm) (Fig. **4-10**).

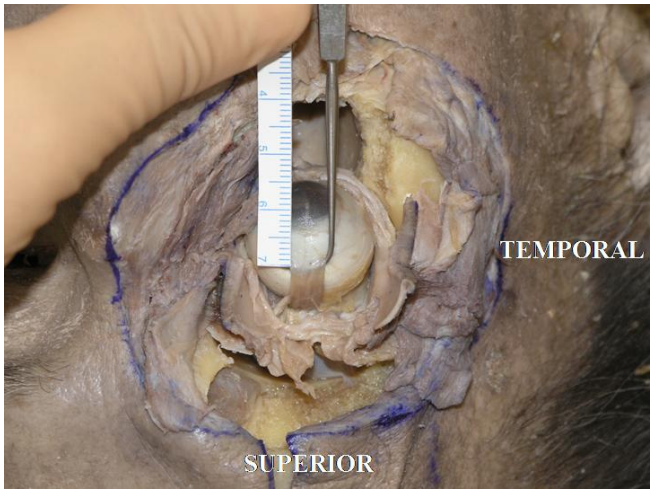

Fig. (4-10). The insertion of the superior rectus muscle tendon is 7.5 mm from the superior corneal limbus.

The insertion is lightly laterally slanted to the limbus. The width in this specimen is about 7.0 mm (Fig. **4-11**).

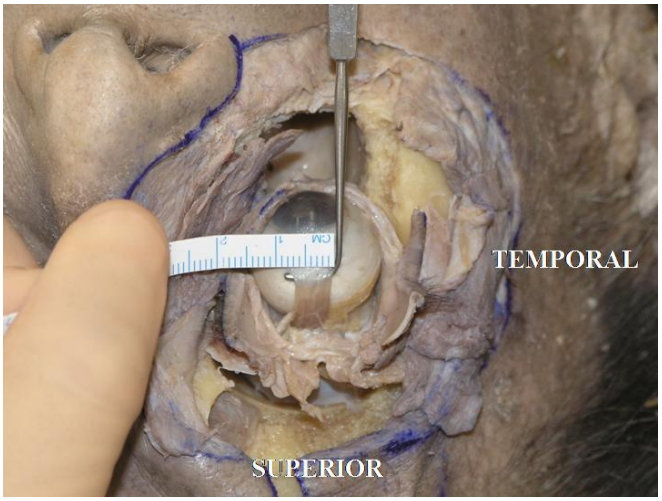

Fig. (4-11). The insertion width of the superior rectus muscle tendon is lightly laterally slanted to the limbus. The width is about 7.0 mm in this specimen.

Detailed Anatomy: There is a controversy regarding the width of the rectus muscle tendons. In Whitnall's textbook [18] the tendon width of the medial rectus muscle is 10.3 mm, that of the inferior rectus muscle is 9.8 mm, the lateral rectus muscle is 9.2 mm and that of the superior rectus muscle is 10.6 mm. Dutton's anatomical textbook presents similar values [41]. On the other hand, in Snell and Lemp's textbook [42] the tendon width of the medial rectus muscle is 3.7 mm, that of the inferior rectus muscle is 5.5 mm, that of the lateral rectus muscle is 8.8 mm and that of the superior rectus muscle is 5.8 mm.

I. The recti muscles are disinserted from the globe and the oblique muscles are next analysed. Both oblique muscles are closer to the globe than the corresponding recti muscles.

J. The tendon of the superior oblique muscle inserts on the posterolateral superior hemisphere of the globe in a fan-like fashion [18], in an area around the lateral border of the superior rectus muscle or lightly more laterally (Fig. **4-12**).

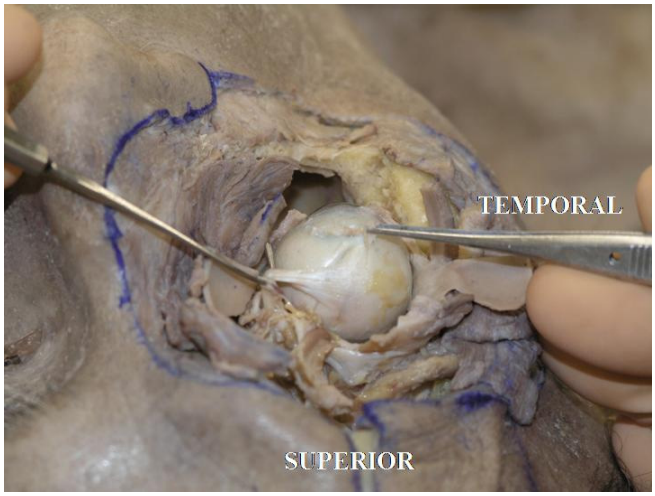

Fig. (4-12). The superior oblique muscle tendon inserts onto the posterolateral superior hemisphere of the globe in a fan-like fashion.

Pulling the tendon may demonstrate the rotational effect on the globe.

K. The inferior oblique muscle tendon inserts on the posterolateral hemisphere of the globe in a fan-like fashion [18], in an area around the superior border of the lateral rectus muscle or lightly more inferiorly (Fig. **4-13**).

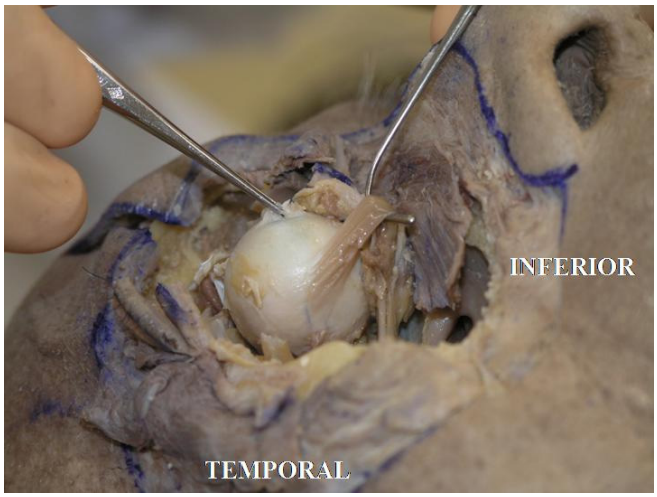

Fig. (4-13). The inferior oblique muscle tendon inserts onto the posterolateral hemisphere of the globe in a fan-like fashion. The tendon is very short.

The tendon is very short. Pulling the tendon may demonstrate the rotational effect on the globe.

L. The insertion of the oblique muscles on the globe is then incised. In this specimen there are several short or long posterior ciliary arteries inserting into the posterior hemisphere of the globe [18] (Fig. **4-14**).

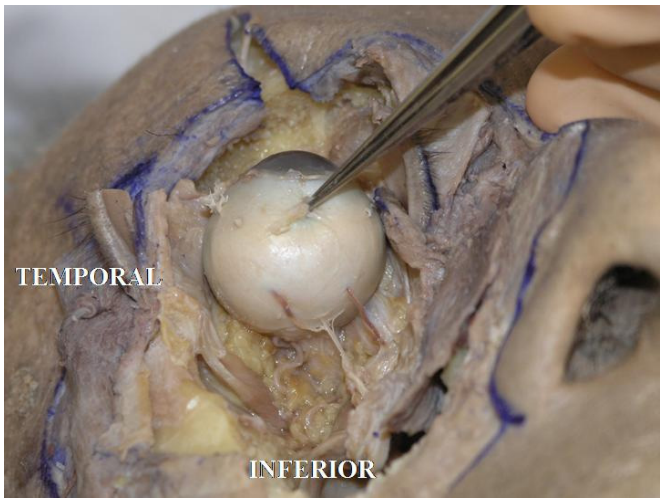

Fig. (4-14). Some short or long posterior ciliary arteries are seen inserting into the posterior hemisphere of the globe.

M. The globe is now removed after cutting the optic nerve. The white optic nerve sheath, optic nerve and large particle orbital fat can be seen [25] (Fig. **4-15**).

Detailed Anatomy: The white optic nerve sheath corresponds to the dura mater and the space between the white sheath and the optic nerve corresponds to the arachnoid filled with cerebrospinal fluid [6].

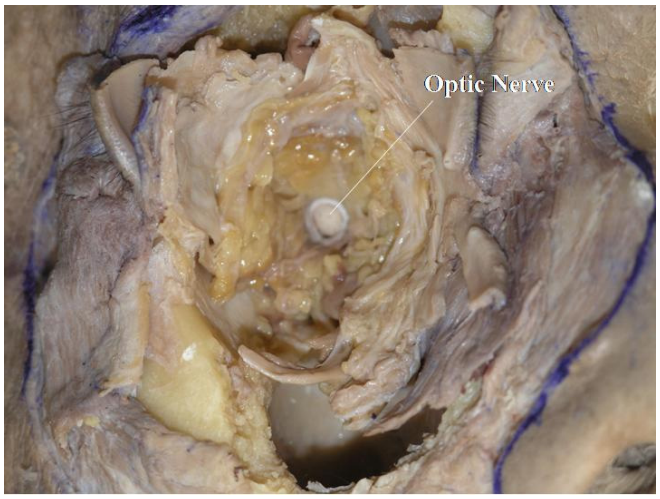

Fig. (4-15). The globe is removed after cutting the optic nerve. The white optic nerve sheath, optic nerve and large particle orbital fat can be seen.

Detailed Anatomy: The orbital fat situated deep in the orbit generally has a larger volume than that in the shallower parts [25].

N. After careful removal of the orbital fat, the insertion of the anterior ciliary arteries can be seen (Fig. **4-16**).

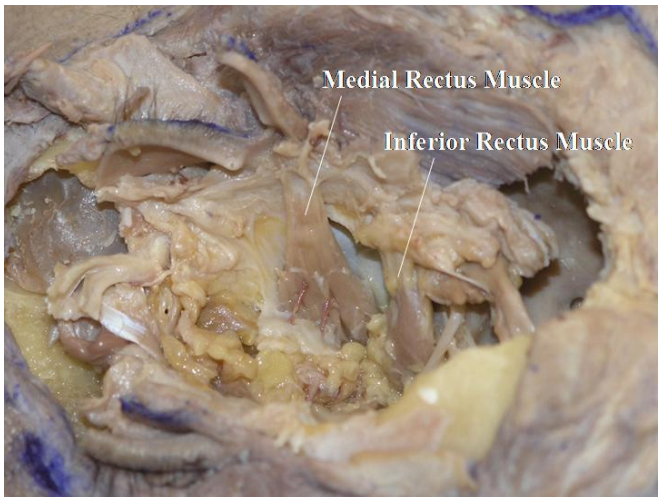

Fig. (4-16). The insertions of the anterior ciliary arteries can be seen.

Detailed Anatomy: The medial, inferior and superior recti muscles receive two anterior ciliary arteries, whereas the lateral rectus muscle receives only one such artery [18].

Detailed Anatomy & Clinical Hint: The anterior ciliary arteries eventually reach the iris and connect to the major arterial circle of the iris [18]. Therefore, a maximum number of two muscles can be operated during a single session of strabismus surgery, to avoid ocular ischemia [43].

O. In this specimen it is possible to visualize the neuromuscular junction of the extraocular muscles. However, as it may take several hours to expose the neuromuscular junctions by removing the orbital fat, this is performed after the dissections of the medial and lateral canthi.

P. The medial canthus is analysed next. From a lateral view, Horner's muscle is shown to originate from the posterior lacrimal crest or even deeper [24] (Fig. **4-17**).

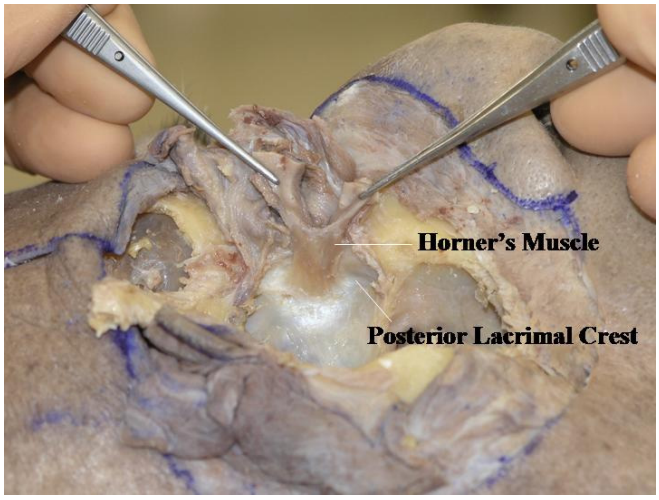

Fig. (4-17). From a lateral view, Horner's muscle is shown to originated from the posterior lacrimal crest or even deeper.

The origin of Horner's muscle is almost parallel to the anterior lacrimal crest. It attaches to the bone more in the upper area but less in the lower area. The lower part of the lacrimal sac (nasolacrimal duct) is not covered by Horner's muscle. Horner's muscle continues to the tarsal plate. When pulling this muscle rhythmically, a hard sensation can be felt from its origin, however no ligamentous structure can be seen.

Q. When the lacrimal sac is incised vertically, the attachment of Horner's muscle to the posterior part of the lacrimal sac can be seen (Fig. **4-18**).

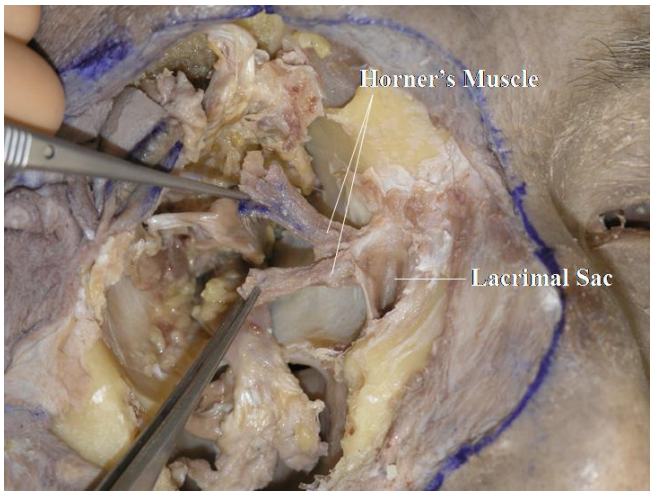

Fig. (4-18). When the lacrimal sac is incised vertically, the attachment of Horner's muscle to the posterior part of the lacrimal sac can be seen.

Clinical Hint: This attachment plays an important role in the dynamic process of lacrimal drainage [24].

R. By inserting a lacrimal probe into the canaliculus, the common internal ostium can be visualized at the centre of Horner's muscle attachment to the lacrimal sac (Fig. **4-19**).

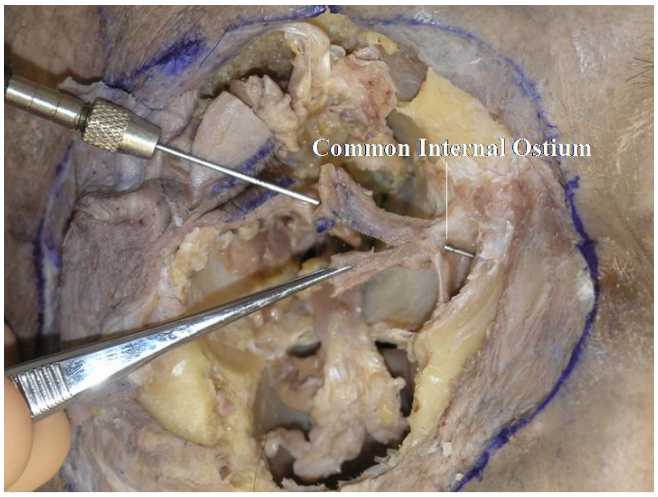

Fig. (4-19). The common internal ostium can be visualized at the centre of Horner's muscle attachment to the lacrimal sac.

S. After dividing the attachment site of Horner's muscle to the lacrimal sac, a fibrous tissue can be seen, which is part of the lacrimal diaphragm [44] (Fig. **4-20**).

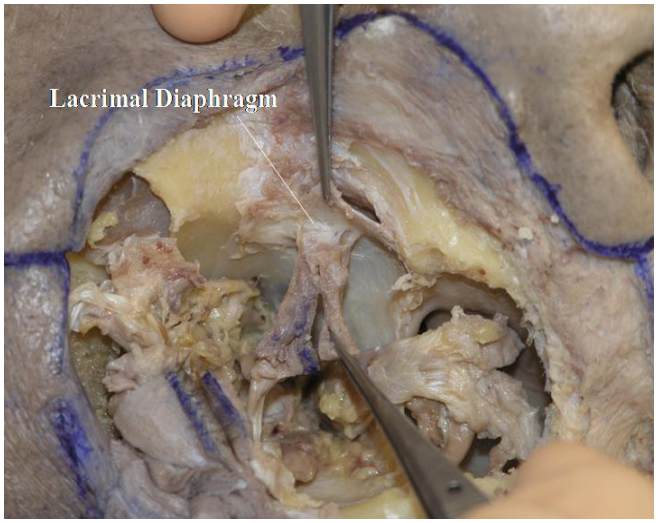

Fig. (4-20). The lacrimal diaphragm is seen on the attachment site of Horner's muscle to the lacrimal sac.

T. At the next stage, the lateral canthus is analysed. The OOM is bluntly detached from the lateral orbital rim. The thickened fibrous tissue on the bone is called the "lateral orbital thickening" (LOT) [28] (Fig. **4-21**).

Detailed Anatomy: The LOT supports the OOM from behind. The area of the LOT becomes smaller with aging [28].

U. The posterior aspect of the OOM and the remaining LOT can be seen (Fig. **4-22**).

V. Analysing the connection between the lateral rectus muscle and the lateral canthus (Fig. **4-23**).

The LCB is seen originating from the shallow part of the lateral orbital rim (Whitnall's tubercle) (Fig. **4-24**).

Here, the lrCPF is shown to have a connection to the LCB.

Fig. (4-21). The thickened fibrous tissue on the bone is called the "lateral orbital thickening".

Fig. (4-22). The remaining of the lateral orbital thickening is seen.

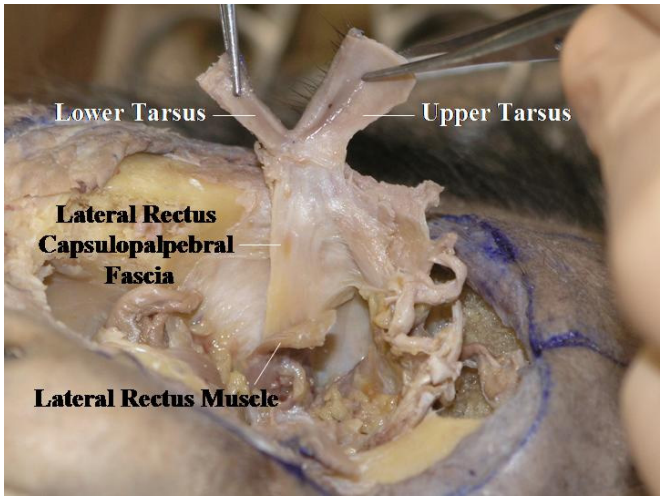

Fig. (4-23). The connection between the lateral rectus muscle and the lateral canthus is shown.

Fig. (**4-25**) shows the frontal view of the LCB. The lateral horn of the levator aponeurosis attaches to the LCB as a part of the lateral retinaculum.

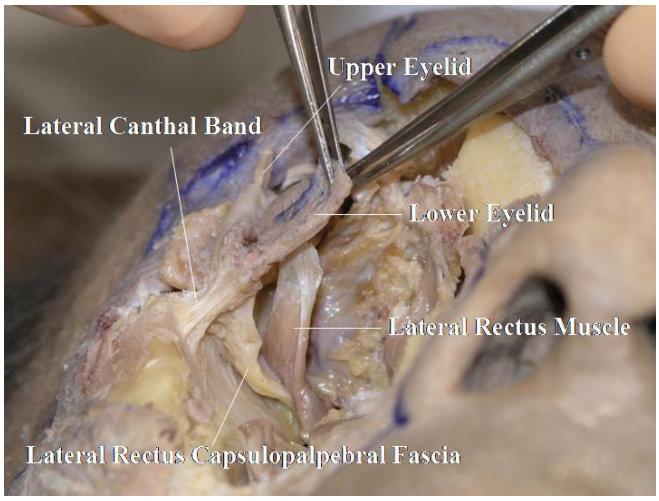

Fig. (4-24). The lateral canthal band (LCB) is shown to originate from Whitnall's tubercle. In this specimen, the lrCPF is seen to have a connection to the LCB.

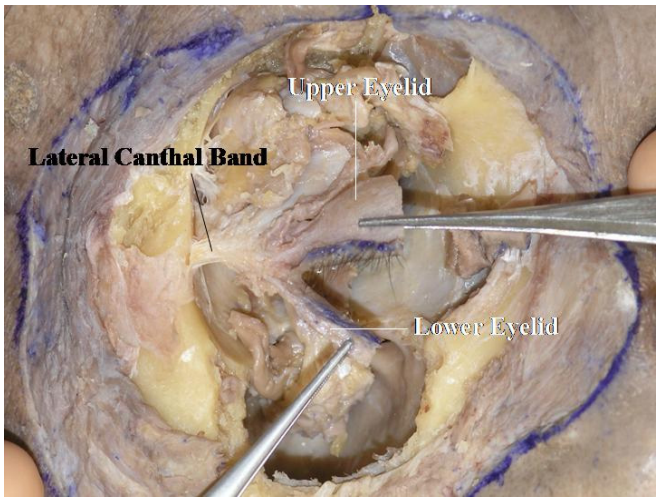

Fig. (4-25). A frontal view of the LCB.

Detailed Anatomy & Clinical Hint: The lateral retinaculum is a supporting structure of the lateral canthus [25]. It contains, (starting superiorly); Whitnall's ligament, ITL, the lateral horn of the levator aponeurosis, the lateral check ligament, LCB and Lockwood's ligament. The lateral retinaculum attaches to Whitnall's tubercle. Although the lateral retinaculum is a strong structure, long term repetitive blinking may cause loosening with lateral canthal rounding.

5. Analyzing of the Neuromuscular Junction of the Extraocular Muscles

As a final step in the dissection, the neuromuscular junctions of the extraocular muscles are analysed. This step should be done in a meticulous fashion, and requires a prolonged exposure process. The fat should be removed piece by piece. Delicate dissection is required to allow the exposure of the thin oculomotor nerve to the LPS muscle.

Before starting this step in dissection, the medial and lateral canthal tissues as well as the lacrimal sac and nasal lacrimal duct should be completely removed. The shape of the lacrimal fossa can be seen here.

It is possible here to see the blood vessels and nerves of the orbit, including the ciliary ganglion.

The nerves to the extraocular muscles arise laterally from the optic nerve (Fig. **5-1**), corresponding to the location of the superior orbital fissure which is located lateral to the optic foramen.

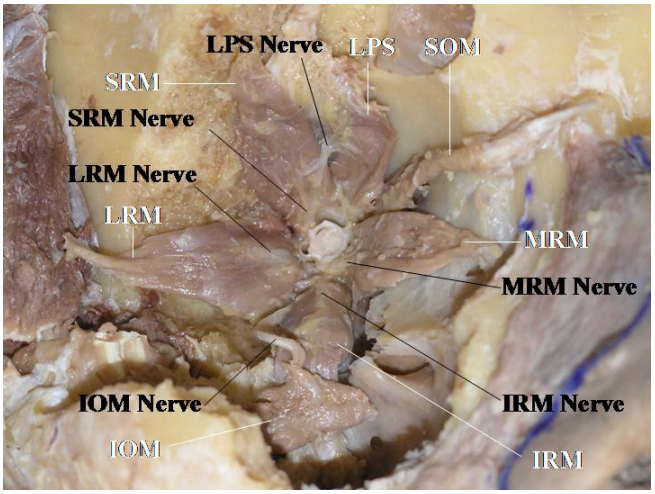

Fig. (5-1). The neuromuscular junctions of the extraocular muscles are shown. SRM: superior rectus muscle, LRM: lateral rectus muscle, IOM: inferior oblique muscle, LPS: levator palpebrae superioris muscle, SOM: superior oblique muscle, MRM: medial rectus muscle, IRM: inferior rectus muscle.

The oculomotor nerve to the medial rectus muscle travels under the optic nerve (Fig. **5-1**). The oculomotor nerve to the inferior oblique muscle travels along the lateral side of the inferior rectus muscle and inserts into the muscle belly on the optic nerve side, in an area between the inferior oblique muscle and the inferior rectus muscle [45, 46] (Fig. **5-1**).

All the neuromuscular junctions, except that of the superior oblique muscle, are located on the optic nerve side. The trochlear nerve inserts into the muscle from superiorly on the orbital wall side [45, 46] (Fig. **5-2**).

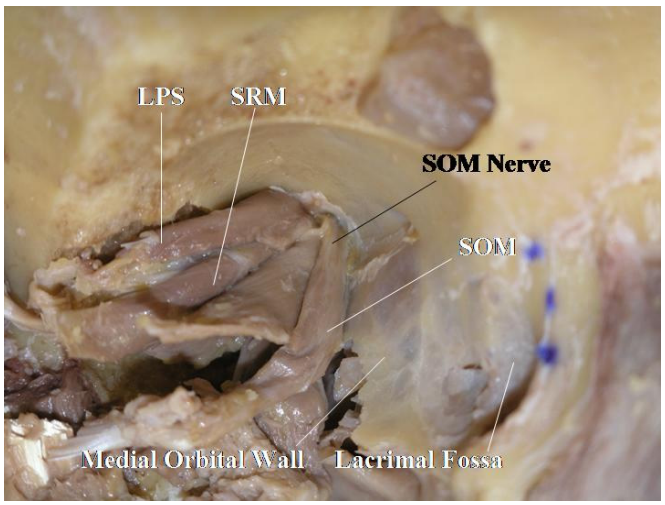

Fig. (5-2). Only the trochlear nerve inserts into the orbital wall side.

The oculomotor nerve to the LPS muscle travels initially with the oculomotor nerve to the superior rectus muscle (superior branch of the oculomotor nerve), but branches off medially to travel further anteriorly to reach the LPS muscle [10, 45, 46] (Fig. **5-2**). The neuromuscular junctions of the extraocular muscles are located in the posterior third of the muscle, but only that of the LPS muscle is at the anterior half of the muscle [10, 44-47].

The ophthalmic artery is seen lateral to the optic nerve during the dissection process (Fig. **5-1**). It arises from the optic canal, inferior to the optic nerve, and generally surpasses the optic nerve from above, travelling forward [6].

CONCLUSION

As the number of cadavers for dissection is very limited, systematic anatomical dissections will maximize their teaching benefit. We hope that this teaching article may provide anatomists and ophthalmologists with sufficient information on techniques of eyelid and orbital dissections with modernised anatomical findings.

REFERENCES

[1] Kakizaki H, Zako M, Mito H, *et al*. The medial canthal tendon is composed of anterior and posterior lobes in Japanese eyes and fixes the eyelid complementarily with Horner's muscle. Jpn J Ophthalmol 2004; 48: 493-6.

[2] Anderson RL. Medial canthal tendon branches out. Arch Ophthalmol 1977; 95: 2051-2.

[3] Kakizaki H, Zako M, Nakano T, *et al*. No raphe identified in the orbicularis oculi muscle. Okajimas Folia Anat Jpn 2004; 81: 93-6.

[4] Goold L, Kakizaki H, Malhotra R, Selva D. Absence of lateral palpebral raphe in Caucasians. Clin Ophthalmol 2009; 3: 391-3.

[5] Stedman's Medical dictionary, 27th ed. Philadelphia: Lippincott Williams & Wilkins 2000; p.1518.

[6] Bron AJ, Tripathi RC, Tripathi BJ. Wolff's anatomy of the eye and orbit. 8th ed. London: Chapman & Hall Medical 1997; pp. 30-84, 85-106, 512-3.

[7] Kikkawa DO, Lemke BN. Orbital and eyelid anatomy. In: Dortzbach RK, Ed. Ophthalmic plastic surgery - prevention and management of complications. New York: Raven Press 1994; pp. 1-29.

[8] Wobig JL, Wilson MW. Eyelid and facial anatomy. In: Putterman AM, Warren LA, Eds. Cosmetic oculoplastic surgery - eyelid, forehead, and facial techniques. Philadelphia: W.B. Saunders Company 1998; pp. 51-66.

[9] Kakizaki H, Zako M, Nakano T, *et al*. Lateral canthal support system in Japanese. Okajimas Folia Anat Jpn 2006; 83: pp. 85-90.

[10] Kakizaki H, Malhotra R, Selva D. Upper eyelid anatomy: an update. Ann Plast Surg 2009; 63: 336-43.

[11] Yuzuriha S, Matsuo K, Kushima H. An anatomical structure which results in puffiness of the upper eyelid and a narrow palpebral fissure in the Mongoloid eye. Br J Plast Surg 2000; 53: 466-72.

[12] Kakizaki H, Zako M, Nakano T, Iwaki M, Mito H. Anatomical study of the lower-positioned transverse ligament. Br J Plast Surg 2004; 57: 370-2.

[13] Kakizaki H, Zako M, Iwaki M, Nakano T, Mito H. Modified course of the lower-positioned transverse ligament. Br J Plast Surg 2005; 58: 1035-6.

[14] Takahashi Y, Kakizaki H, Kinoshita S, Iwaki M. Histological analysis of the lower-positioned transverse ligament. Open Ophthalmol J 2007; 1: 17-9.

[15] Kakizaki H, Zako M, Nakano T, Asamoto K, Miyaishi O, Iwaki M. Medial horn supporting ligament in Asian upper eyelids. Orbit 2008; 27: 91-6.

[16] Kakizaki H, Leibovitch I, Selva D, Asamoto K, Nakano T. Orbital septum attachment on the levator aponeurosis in asians *in vivo* and cadaver study. Ophthalmology 2009; 116: 2031-5.

[17] Kakizaki H, Zako M, Miyaishi O, Nakano T, Asamoto K, Iwaki M. Posterior aspect of the orbital septum is reinforced by ligaments. Jpn J Ophthalmol 2005; 49: 477-80.

[18] Whitnall SE. Anatomy of the human orbit and accessory organs of vision (reprint). London: Robert E. Krieger Publishing Company 1979; pp. 13-4, 269-71, 307-8.

[19] Lukas JR, Priglinger S, Denk M, Mayr R. Two fibromuscular transverse ligaments related to the levator palpebrae superioris: Whitnall's ligament and an intermuscular transverse ligament. Anat Rec 1996; 246: 415-22.

[20] Ettl A, Priglinger S, Kramer J, Koornneef L. Functional anatomy of the levator palpebrae superioris muscle and its connective tissue system. Br J Ophthalmol 1996; 80: 702-7.

[21] Kakizaki H, Zako M, Nakano T, Asamoto K, Mito H, Iwaki M. Intermuscular transverse ligament goes under the orbital part of the lacrimal gland and attaches to the lateral orbital wall. Jpn J Ophthalmol 2005; 49: 542-3.

[22] Lockwood CB. The anatomy of the muscles, ligaments, and fasciae of the orbit, including an account of the capsule of Tenon, the check ligaments of the recti, and of the suspensory ligament of the eye. J Anat Physiol 1885; 20: 1-25.

[23] Kakizaki H, Zako M, Nakano T, Asamoto K, Miyaishi O, Iwaki M. Direct insertion of the medial rectus capsulopalpebral fascia to the tarsus. Ophthal Plast Reconstr Surg 2008; 24: 126-30.

[24] Kakizaki H, Zako M, Miyaishi O, Nakano T, Asamoto K, Iwaki M. The lacrimal canaliculus and sac bordered by the Horner's muscle form the functional lacrimal drainage system. Ophthalmology 2005; 112: 710-6.

[25] Kakizaki H, Malhotra R, Madge SN, Selva D. Lower eyelid anatomy: an update. Ann Plast Surg 2009; 63: 344-51.

[26] Bartley GB, Gerber TC. Eisler and his pocket. Am J Ophthalmol 2006; 141: 417-8.

[27] Kikkawa DO, Lemke BN, Dortzbach RK. Relations of the superficial musculoaponeurotic system to the orbit and characterization of the orbitomalar ligament. Ophthalmol Plast Reconstr Surg 1996; 12: 77-88.

[28] Muzaffar AR, Mendelson BC, Adams WP, Jr. Surgical anatomy of the ligamentous attachments of the lower lid and lateral canthus. Plast Reconstr Surg 2002; 110: 873-84.

[29] Kakizaki H, Zako M, Nakano T, Asamoto K, Miyagawa T, Iwaki M. Three ligaments reinforce the lower eyelid. Okajimas Folia Anat Jpn 2004; 81: 97-100.

[30] Hawes MJ, Dortzbach RK. The microscopic anatomy of the lower eyelid retractors. Arch Ophthalmol 1982; 100: 1313-8.

[31] Murakawa K. Trigeminal nerve block. In: Kishimoto S, Ed. Practical otolaryngology 8. Tokyo: Bunkodo, 2002; pp. 244-50 (Japanese).

[32] Kakizaki H, Zako M, Nakano T, Asamoto K, Miyaishi O, Iwaki M. Microscopic findings of lateral tarsal fixation in Asians. Ophthal Plast Reconstr Surg 2008; 24:131-5.

[33] Kakizaki H, Selva D, Leibovitch I. Dynamic study of the medial and lateral recti capsulopalpebral fasciae using cine mode magnetic resonance imaging. Ophthalmology 2009; [Epub ahead of print].

[34] Lipham WJ, Tawfik HA, Dutton JJ. A histologic analysis and three-dimensional reconstruction of the muscle of Riolan. Ophthalmol Plast Reconstr Surg 2002; 18: 93-8.

[35] Kakizaki H, Jinsong Z, Zako M, *et al*. Microscopic anatomy of Asian lower eyelids. Ophthalmol Plast Reconstr Surg 2006; 22: 430-3.

[36] Lim WK, Rajendran K, Choo CT. Microscopic anatomy of the lower eyelid in asians. Ophthalmol Plast Reconstr Surg 2004; 20: 207-11.

[37] Kakizaki H, Malhotra R, Nakano T, *et al*. Medial and lateral horns of the lower eyelid retractors. Ophthalmol Plast Reconstr Surg 2009; 25: 10-2.

[38] Kakizaki H, Zhao J, Nakano T, *et al*. The lower eyelid retractor consists of definite double layers. Ophthalmology 2006; 113: 2346-50.

[39] Kakizaki H, Chan W, Madge SN, Malhotra R, Selva D. Lower eyelid retractors in Caucasians. Ophthalmology 2009; 116: 1402-4.

[40] Kakizaki H, Iwaki M. A new trapezoid lower eyelid clamp to shape the lower conjunctival fornix. Eur J Plast Surg 2008; 31: 161-4.

[41] Dutton JJ. Clinical and surgical orbital anatomy. Philadelphia: W.B. Saunders Company 1994; pp. 16-9.

[42] Snell RS, Lemp MA. In: Inomarta H, Ed. Clinical anatomy of the eye. Oxford: Blackwell Scientific Publications, Inc, 1989. Japanese version. Tokyo: Igakushoin 1993: pp. 217-56.

[43] Nardi M. Eye muscle surgery. In Wiersinga WM, Kahaly GJ, Eds. Graves' orbitopathy-a multidisciplinary approach. Basel: Karger, 2007; pp. 176-87.

[44] Jones LT. Epiphora II: its relation to the anatomic structures and surgery of the medial canthal region. Am J ophthalmol 1957; 43: pp. 203-12.

[45] Kakizaki H, Zako M, Nakano T, Asamoto K, Miyagawa T, Iwaki M. Myoneural junctions of extraocular muscles: distances from the orbital rim and widths. Ophthalmologica 2006; 220: pp. 87-93.

[46] Kakizaki H, Zako M, Miyagawa T, Nakano T, Asamoto K, Iwaki M. Myoneural junctions of extraocular muscles: distances from the orbital rim and widths. Part 2. Ophthalmologica 2006; 220: 347.

[47] Hwang K, Lee DK, Chung IH, Lee SI. Patterns of oculomotor nerve distribution to the levator palpebrae superioris muscle, and correlation to temporary ptosis after blepharoplasty. Ann Plast Surg 2001; 47; pp. 381-4.

Received: September 18, 2009 Revised: November 4, 2009 Accepted: November 14, 2009